We are IntechOpen, the world's leading publisher of Open Access books Built by scientists, for scientists

6,900
Open access books available

185,000
International authors and editors

200M
Downloads

Our authors are among the

154
Countries delivered to

TOP 1%
most cited scientists

12.2%
Contributors from top 500 universities

WEB OF SCIENCE™

Selection of our books indexed in the Book Citation Index in Web of Science™ Core Collection (BKCI)

Interested in publishing with us?
Contact book.department@intechopen.com

Numbers displayed above are based on latest data collected.
For more information visit www.intechopen.com

11

Clinical Applications of Rapid Prototyping Models in Cranio-Maxillofacial Surgery

Olszewski Raphael and Reychler Hervé
Université catholique de Louvain
Belgium

1. Introduction

Medical models or bio-models represent portions of human anatomy at a scale of 1:1 obtained from three-dimensional (3D) medical imaging (CT scan, MRI). The procedure for the fabrication of medical models consists of multiple steps: 1) the acquisition of high-quality volumetric 3D image data of the anatomical structure to be modelled, 2) 3D image processing to extract the region of interest from surrounding tissues, 3) mathematical surface modelling of the anatomic surfaces, 4) formatting of data for rapid prototyping (RP) (this includes the creation of model support structures that support the model during building, which are subsequently manually removed), 5) model building, and 6) quality assurance of the model and its dimensional accuracy. These steps require significant expertise and knowledge of medical imaging, 3D medical image processing, computer-assisted design, and software manufacturing and engineering processes. The production of reliable, high-quality models requires a team of specialists that may include medical imaging specialists, engineers, and surgeons (Winder & Bibb, 2005). Rapid prototyping was introduced in the 1980's to define new techniques for the manufacturing of physical models based on CAD-CAM (computer-aided design, computer-aided manufacturing). RP technology allows the building of a medical model layer by layer, reproducing almost every form of the external and internal anatomic structure. Other categories of RP technologies are solid freeform fabrication, layer additive manufacturing, and 3D printing. RP techniques are different from physical models obtained by milling. RP medical modelling in cranio-maxillofacial (CMF) surgery has mainly been developed over the last ten years (Phidias European network), and concerns the following range of applications: 1) aiding in the production of surgical implants, 2) improving surgical planning, 3) acting as an orientation aid during surgery, 4) enhancing diagnostic quality, 5) using in preoperative simulation, 6) achieving a patient's consent prior to surgery, and 7) preparing a template for resection for surgeons (Winder & Bibb, 2005).

2. Review of current RP techniques in CMF surgery

2.1 Introduction

Almost all of the RP techniques that have been described were developed to construct 3D medical models for CMF surgery, and these will be presented in the following literature review. These techniques include stereolithography (SL), selective laser sintering (SLS), fused deposition modelling (FDM), 3D printing (3DP), and polyjet modelling.

2.2 Materials and method

A systematic review of the literature was conducted on PubMed (Medline). A search strategy employed was based on title-abstract sifting by one observer. Our exclusion criteria consisted of general dentistry, prosthodontics, orthodontics, forensic medicine, orthopaedics, biomechanics, finite element analysis, and virtual imaging. The inclusion criteria consisted of medical rapid prototyping, three-dimensional models, stereolithography, selective laser sintering, fused deposition modelling, 3D printing, polyjet, maxillofacial, craniofacial, cranioplasty, implantology. The search strategy was based on eight search equations that combined free terms and MeSh terms: 1) ((RP[All Fields] AND models[All Fields]) AND maxillofacial[All Fields] AND ("humans"[MeSH Terms] AND English[lang])) (search on 15.03.11), with 10 articles found, and 10 articles selected; 2) ((Medical[All Fields] AND rapid[All Fields] AND prototyping[All Fields]) AND (maxillofacial[All Fields] OR craniofacial[All Fields]) AND ("humans"[MeSH Terms] AND English[lang])) (search on 17.03.11), with 19 articles found, and 19 articles selected; 3) ((three-dimensional[All Fields] AND models[All Fields]) AND (maxillofacial[All Fields] OR craniofacial[All Fields]) AND ("humans"[MeSH Terms] AND English[lang])) (search on 17.03.11 to 19.03.11), with 450 articles found, 350 articles excluded, and 100 articles selected; 4) ((stereolithography[All Fields] AND maxillofacial[All Fields] AND ("humans"[MeSH Terms] AND English[lang])) (search on 15.03.11), with 37 articles found, 6 articles excluded, and 31 articles selected; 5) ((Selective laser sintering [All Fields] AND maxillofacial[All Fields] AND ("humans"[MeSH Terms] AND English[lang])) (search on17.03.11), with 9 articles found, 1 article excluded, and 8 articles selected; 6) (fused deposition modelling [All Fields] AND maxillofacial[All Fields] AND ("humans"[MeSH Terms] AND English[lang])) (search on 17.03.11), with 1 article found, and 1 article selected; 7) ((three[All Fields] AND dimensional[All Fields]) AND (printer[All Fields] OR ("printing"[MeSH Terms] OR "printing"[All Fields])) AND maxillofacial[All Fields] AND ("humans"[MeSH Terms] AND English[lang]) (search on 15.03.11), with 7 articles found, 1 article excluded, and 6 articles selected; and 8) (polyjet[All Fields] AND (maxillofacial[All Fields] OR craniofacial[All Fields]) AND ("humans"[MeSH Terms] AND English[lang]) (search on 17.03.11), with 1 article found, and 1 article selected. The limits were human studies and English language. There were no limits for the time of publication. The total number of articles found was 534, with 365 articles excluded, and 169 articles selected. The number of duplicate article found among the eight search equations was 42.

After title-abstract sifting, 127 articles were retained. There were 25 articles excluded after reading of the articles. There were also 3 redundant publications. Finally, we selected 99 articles for review.

2.3 Discussion

2.3.1 Stereolithography

SL has been the most used RP technique in CMF surgery since it was first applied in grafting a skull defect in 1994 (Mankovich et al., 1994).

2.3.1.1 Technique

An SL RP system consists of a bath of photosensitive resin, a model-building platform, and an ultraviolet (UV) laser for curing the resin. A mirror is used to guide the laser's focus onto the surface of the resin, where the resin becomes cured when exposed to UV radiation. The mirror is computer- controlled, with its movement being guided to cure the resin on a slice-

by-slice basis. A model is initially designed with CAD software in a suitable file format (commonly STL) and transferred to the SL machine for building. The CAD data file is converted into individual slices of known dimensions. These slice data are then fed into the RP machine, which guides the exposure path of the UV laser onto the surface of the resin. The layers are cured sequentially and bond together to form a solid object beginning from the bottom of the model and building upward. As the resin is exposed to the UV light, a thin, well-defined layer becomes hardened. After a layer of resin is exposed, the resin platform is lowered within the bath by a small known distance. A new layer of resin is wiped across the surface of the previous layer using a wiper blade, and this second layer is subsequently exposed and cured. The process of curing and lowering the platform into the resin bath is repeated until the full model is complete. The self-adhesive property of the material causes the layers to bond to each other and eventually form a complete, robust, 3D object. The model is then removed from the bath and cured for an additional period of time in a UV cabinet. The built portion may contain layers, that significantly overhang layers below. If this is the case, then a network of support structures, made of the same material, is added beneath the overhanging layers at the design stage to add support during the curing process. These support structures, analogous to a scaffold, are removed by hand after the model is fully cured, which is a labour-intensive and time-consuming process. Generally, SL is considered to provide the greatest accuracy and best surface finish of any RP technology. The model material is robust, slightly brittle, and relatively light, although it is hydroscopic and may physically warp over time (a few months) if exposed to high humidity (Ono et al., 1994; Choi et al, 2002; Winder & Bibb, 2005).

2.3.1.2 Clinical applications

SL models have been used as preoperative planning tools in CMF traumlatology, CMF surgery for craniofacial syndromes and the correction of asymmetric faces, orthognathic surgery, distraction osteogenesis, CMF post-tumoral reconstructive surgery, temporomandibular joint surgery, skull defects reconstruction and cranioplasty, and implantology. This technique can also be used for ear or orbital reconstruction and could be potentially applied in anthropological studies or in the study of facial aging (Papadopoulos et al., 2002). Selectively colored SL models have also been used for the diagnosis and planning of treatments related to supernumerary teeth extraction in cleidocranial dysplasia (Sato et al., 1998), in planning a complex maxillofacial tumour surgery (Kermer et al., 1998), and for the visualisation of rapports between the disc and mandibular condyle in the tempormandibular joint (Undt et al., 2000).

SL models may assist in the diagnosis of and preoperative planning for facial fractures, especially in late primary repair, when open reduction and internal fixation have to wait for a decrease in facial swelling or cerebral oedema. SL models facilitate anatomical reduction, minimise surgical approaches, save operating time, and lead to improvement of postoperative results, which may reduce the number of secondary corrections required for post-traumatic deformities (Kermer et al., 1998; Powers et al., 1998). Post-traumatic deformities after fractures of the zygomatic complex are seen less often in the age of routine open reduction and rigid fixation; nevertheless, they can occur because of diagnostic and therapeutic failures. In the case of delayed reconstruction, the surgeon has to cope with the patients' functional symptoms (diplopia, hypoesthesia, and reduced mouth opening), as well as aesthetic challenges. The repositioning of the entire zygomatic complex is a method that promises the complete reversal of all symptoms. However, this method represents the

most difficult part of the surgery because of the limited access to the region. As a consequence of remodelling processes, no obvious edges of a fracture remain that could serve as landmarks to determine correct positioning (Klug et al., 2006). An SL model allows for analysis of the actual displacement of bone in all 3 dimensions. Additionally, SL models can be employed to plan a surgery and move the zygoma to its final ideal position. Using these models, osteosynthesis plates can be individually pre-bent before actual surgery, thereby shortening operating time. To transfer the preoperative plan to the operating theatre, a 3D- CT-based navigation system can be associated with SL models to transfer the exact positions of the screws from the SL model to the patient (Klug et al., 2006). However, SL models have proven to be less useful in cases of consolidated fractures of the periorbital and naso-ethmoidal complex, except where there is major dislocation, because of the limited representation of detailed structures (sutures) present in this region (Sailer et al., 1998).

A surgery can be simulated in SL models prior to operation on malformative craniofacial syndromes, in which the visualisation of complex anatomy may considerably modify the surgical approach applied, as well as avoiding unnecessary complications (Pelo et al., 2006; Sinn et al., 2006). SL models have provided additional relevant anatomical information for surgeons related to hypertelorism, severe asymmetries of the neuro- and viscerocranium (Wong et al., 2005), complex cranial synostoses and large skull defects. For hemifacial microsomia (unilateral hypoplasia of the craniofacial skeleton and its overlying soft tissue), Zhou et al. (Zhou et al., 2009) developed a customised mandibular implant model that was designed in a computer-assisted manner by projecting a mirror image of the healthy mandible onto the affected side in a three-dimensional CT model. A resin SL model of the implant was then made using a RP machine. Finally, a polymeric biomaterial was sculpted according to the SL model and implanted into the affected side of the mandible to restore the patient's facial symmetry (Chang et al., 1999; Wong et al., 2005; Zhou et al., 2009). The value of these models as realistic "duplicates" of complex or rare dysmorphic craniofacial pathologies for the purpose of creating a didactic collection should also be emphasised (Sailer et al., 1998). However, SL models representing only bone do not reveal the spatial relationships between soft tissue and bone in complicated craniofacial deformities. Therefore, a mixed SL model has been developed showing both soft and bony tissue by first using CT values, resulting in a model in which soft tissue is solid and bone is replaced by empty space (Nakajima et al., 1995). The space is then filled with plaster to represent the skeleton. This model also can provide baseline data for evaluating facial growth after surgical repair of clefts (Nakajima et al., 1995; Al-Ani et al., 2008).

The aim of orthognathic surgery is to treat sagittal, vertical or transverse skeletal congenital or post-traumatic dysmorphoses, based on different types of osteotomies of the maxilla/and or mandible, and to modify the relative position of the maxilla to the mandible, and the absolute position of both the maxilla and mandible to the skull base. Orthognathic surgery is almost associated with pre- and post- surgery orthodontic treatement, as the stable occlusion between the jaws is one of the main goals of the treatment. In orthognathic surgery, SL models replicate the facial skeleton with precise internal anatomy, which can facilitate the design of the osteotomy and the preparation for osteosynthesis. Each sectioned segment of the maxilla and mandible can be accurately repositioned by transferring the positional relationships of multiple reference points on the SL model to the bone surface using pre-bent titanium plates (Hibi et al., 1997). Efforts have been made to replace CT-images, which are often affected by artefacts (due to metallic dental amalgams), thus resulting in poor representation of the tooth area in SL models, as occlusion plays a major

role in orthogntahic surgery in terms of aestehics, and in avoiding postoperative relapse. Therefore, hybrid SL models based on scanning of plaster casts and on skull CTs have been obtained to allow for more accurate planning of orthognathic surgeries (Hoffmann et al., 2002). The SL technique allows the generation of digital templates that are used during surgery to assist the surgeon in repositioning the maxilla and/or the mandible in relation to each other (Gateno et al., 2007).

Distraction osteogenesis is a surgical process used to reconstruct skeletal deformities and lengthen long bones of the body. A corticotomy is used to fracture the bone into two segments, and the two ends of the bone are gradually drawn (with a distraction device) apart during the distraction phase, allowing new bone to form in the gap. When the desired or possible length is reached, a consolidation phase follows, in which the bone is allowed to continue healing. Distraction osteogenesis has the benefit of simultaneously increasing bone length and the volume of surrounding soft tissues. Its application to the craniofacial skeleton allowed for better corrections of multiple complex maxillo-mandibular craniofacial deformities to be achieved. SL models have been used preopeatively to evaluate various surgical solutions (Whitman & Connaughton, 1999; Robiony et al., 2007), simulate osteotomies, simulate the positioning of the distractor device (Poukens et al., 2003), prebend plates or inserts of the distraction device (Minami et al., 2007; Varol & Basa, 2009), define the vector of distraction (the direction of the movement of the elongated bone), simulate final results (Yamaji et al., 2004; Robiony, 2010), and to develop a surgical guide to transfer a surgical plan (osteotomy lines, and the positions of inserts on both sides of the distracted area) to the operating theatre (Poukens et al., 2003). If the distractor is to be prepared for mandibular elongation, the position of the screws (inserts) can be determined preoperatively according to growth trends and the location of the tooth buds and inferior alveolar nerve (Feiyun et al., 2010). In correcting mandibular micrognathia and tempormandibular joint (TMJ) ankylosis in particular, 3D SL models have several advantages: 1) the range of bilateral TMJ ankylosis and the position of the osteotomy line can be easily determined; 2) the transport disc can be designed at the posterior edge of the mandibular ramus, with individual, tailored ramus distractors being made; 3) the precise distraction length of the bilateral mandible body can be determined for later orthodontic therapy and orthognathic surgery; 4) the position of the osteotomy line in the mandible body can be determined, with an individual tailored distractor being made; 5) for immobilisation, the attachment plate of the distractor can be adjusted and attached to the surface of the mandible; and 6) surgical procedures can be explained clearly to patients using the 3D model. Thus, 3D CMF model have great potential in therapy for bilateral TMJ ankylosis accompanied by mandibular micrognathia (Feiyun et al., 2010). However, surgery using an STL model cannot not be repeated, because RP is expensive, and models often become useless after primary model surgery (Varol & Basa, 2009). SL models can be used for preoperative planning of maxillary resection due to oral cancer (Lethaus et al., 2010) and for the planning of maxillary reconstruction with osseo-cutaneous microvascularised free-flaps. A 3D SL model can serve to 1) visualise the extent of a tumour (Eisele et al., 1994); 2) evaluate the anatomy of a defect, and define the residual anchor bone for integration with free-flap segments (He et al., 2009); 3) design osteotomies based on free-flaps and the direction of segment replacement to simulate symmetric maxilla reconstruction (He et al., 2009); 4) fit a graft exactly, with or without reduced reshaping (He et al., 2009); 5) preadapt plates based on a SL model (Al-Sukhun et al., 2008); 6) manufacture a surgical guide for

tumoral resection (Ekstrand & Hirsch, 2008); 7) shorten the surgical time before a free-flap is reanastomosed and reduce the risk of microsurgery (He et al., 2009); 8) predict the outcome of surgery (He et al., 2009); and 9) provide a permanent record for future needs or reconstructions (Eisele et al., 1994).

SL models have also been used for the preoperative planning of mandibular resection and reconstruction (Matsuo et al., 2010). Mandibular reconstruction is often needed after partial resection and due to continuity defects (Cohen et al., 2009). The aims for the reconstruction are maintaining the proper aesthetics and symmetry of the face and achieving of a good functional result, thus preserving the form and the strength of the jaw and allowing future dental rehabilitation (Cohen et al., 2009). Reconstruction poses a challenge for the maxillofacial surgeon for a number of reasons, such as the complicated geometry of the mandible, the muscles attached to the mandible, which act in different directions, the shape and position of the condyles in the glenoid fossa, and occlusion (Cohen et al., 2009). Reconstruction of the mandible can be achieved using a temporary bridging titanium locking bone plate until bony reconstruction of the gap is accomplished (Cohen et al., 2009). The use of the reconstruction plate is also advocated when predicted life expectancy is low and when medical conditions preclude prolonged general anaesthesia (Cohen et al., 2009). Further rehabilitation of the mandible can be performed using autogenous bone grafting (iliac crest, fibula free-flap), which is a reliable standard procedure (Cohen et al., 2009). Incorporation of the bone graft into the mandible provides the continuity and strength necessary for its proper functioning, with the possibility of dental implant rehabilitation (Cohen et al, 2009). Bone tissue can be harvested during the first surgical procedure or at a later stage (Cohen et al., 2009).

SL 3D models of the mandible are used to assist in developing a presurgical plan, including consideration of the length of the resection (Kernan & Wimsatt, 2000). On the SL model, the mandibular and mental foramina are marked, the course of the mental nerve is demarcated, and the boundaries of the mandibular resection are chosen. The reconstruction plate is premolded to the planned neomandible SL model. Intraoperative time is not expended moulding the plate imprecisely. Instead, the plate can be bent as exactly as possible before the operation without the pressure of time. This method serves as a valuable learning tool for junior surgeons. Patients can also gain a significantly better understanding of the problem and the challenges of reconstruction by using such models, which results in a better alignment of hopes and expectations between patients and surgeons. Some potential drawbacks of these techniques include the cost of SL models and the difficulty in adapting them to situations in which the surgical plan changes intraoperatively (ie, tumour-positive bone margins demanding a larger bone resection) (Hirsch et al., 2009). Intraoperative navigation could be associated with the use of SL models to ensure that the locations of mandibular osteotomies coincide with the planning phase (Ewers & Schicho, 2009; Juergens et al., 2009). Plates (Kernan & Wimsatt, 2000), trays (Matsuo et al., 2010), or titanium mesh cages for iliac bone (Yamashita et al., 2008), can be easily bent and adapted to fit a mandibular SL models (Zhou et al., 2010; Kernan & Wimsatt, 2000). SL model also enable the surgeon to determine the required length of a plate, and the length and number of screws (Kernan & Wimsatt, 2000). As a result, before resection, there is an accurately fitted and contoured reconstruction plate ready for placement. Decreased exposure time to general anaesthesia, decreased blood loss, and lessened wound exposure time are all significant patient benefits from reduced operating times (Kernan & Wimsatt, 2000). The ability to complete nonsurgical aspects of a patient's treatment in the laboratory also allows

for precision that is often not achievable during the operative procedure (Kernan & Wimsatt, 2000). A method to transfer a reconstructive plate from an SL model to a patient has been proposed: Two acrylic guides were built (1 for each side) with prints of the occlusal surfaces of the remaining teeth and the titanium plate, allowing the accurate replication of the guide position in the mandibular remnant. This procedure allows for very accurate replication of the 3D position of the plate, without the need for partial resection of the tumour before fixing the plate (Fariña et al., 2009).

Reconstruction of major surgical defects in the oral cavity after oncological resections requires the use of a free flap. Vascularised free fibular flaps are considered the most suitable choice for mandible reconstruction because of their favourable aesthetics and their functional outcomes. Fibular bone allows the planning of osteotomies in relation to the orientation of the bone and to its vascular pedicle. Thick cortical bone readily accepts plates and screws for secure interosseous fixation, and osteointegrated implants may be placed in this bone safely. The length of bone that can be removed is up to 25 cm; the bone may be osteotomised in 2 to 4 fragments, and retains its vitality. Other tissue structures such as the skin, fascia, and muscle, are removed with the bone. A fibula free-flap graft has to be contoured to fit the mandibular defect, so preoperative planning is required. Shaping of the fibular graft can be performed using computer-aided design and computer-aided modelling procedures for evaluation of the presurgical anatomy, whereby 3D SL models of the fibula graft are obtained (Liu et al., 2009). The 3D SL models of the fibula graft allow for selecting the best titanium plates for each case and bending the plates preoperatively, which reduces the time spent in the operating theatre. While the application of computer-assisted maxillofacial surgery is becoming increasingly popular, translation from virtual models and surgical plans to the operating theatre remains a major challenge. Methods have been described to translate virtual plans to surgical applications using an RP guide based on a 3D SL model for resection of the fibula and for its insertion into the resected defect in the mandible (Hirsch et al., 2009). Additioanlly, osteotomies could be translated into surgical situations through an RP guide (Hirsch et al., 2009), and the length of the resected bone, the mandibular curvature, and the width of the basal bone could be transferred to the fibula flap with template modelling (Hirsch et al., 2009).

Finally, SL models have also been used for preoperative planning and to guide the bending of titanium plates to be used in the resection of benign tumours with mandibular bone involvement such as ameloblastoma (Mainenti et al., 2009).

Temporomandibular joint (TMJ) surgery is mainly performed to treat mandibular condyle fractures, degenerative osteoarthritic diseases, congenital aplasia, tempormandibular ankylosis, and tumours. SL models based on CT imaging (Zhang et al., 2011) or MRI (Undt et al., 2000) can help in the visualisation of bony structures and the shape of the articular disc in relation to bony structures (Undt et al., 2000).

SL models can also serve in constructing a custom-made, total TMJ prosthesis that is adapted surgically to a patient's unique anatomy (Worrall & Christensen, 2006; Zizelmann et al., 2010).

Additionally, SL models have been used for patients with skull bony defects requiring corrective cranioplasty after the resection of osseous tumours, with congenital and posttraumatic craniofacial deformities, requiring reconstructive cranioplasty, and requiring planning of difficult skull base approaches (Müller et al., 2003). SL models for corrective cranioplasty allowed for the simulation of osteotomies for advancement plasty and craniofacial reassembly in the model before surgery, thus reducing operating time and

intraoperative errors. The usefulness of SL models in congenital craniofacial deformities depended directly on the size and configuration of the cranial defect. The indications for the manufacture of individual 3D SL models could be cases of craniofacial dysmorphism that require meticulous preoperative planning and skull base surgery with difficult anatomical and reconstructive problems. The SL models provide 1) a better understanding of the anatomy, 2) presurgical simulation, 3) intraoperative accuracy in the localisation of lesions, 4) accurate fabrication of implants, and 5) improved education of trainees (Müller et al., 2003; Wong et al., 2002). A titanium plate can be customised based on an SL model for ideal adaptation to convex (Dattilo & Bursick D, 1994; Arnaud et al, 1997), and/or concave skull defects. The reconstruction of unilateral bony defects was also based on the use of virtual mirror imaging of the side controlateral to the side with the defect. An STL mirror model was then produced that served as a template (Lo et al., 2004) for a cranioplasty implant (Bill et al., 1995). Finally, implants from diverse sources, such as artificial bone (Cao et al., 2010), bone allotransfers (Kübler et al., 1995), and titanium mesh (Wu et al., 2008), were manufactured to fit into cranial defects.

An approach combining computer-aided design, SL models and surgical navigation could help manage complex lesions in the skull base and craniofacial area requiring rigid reconstruction (Wu et al., 2008).

Finally, selectively coloured SL models have been used to construct surgical guides for dental implant placement. The colour allowed for the identification of internal structures, such as the inferior alveolar nerve canal inside the mandible or maxillary sinuses inside the maxilla. It is of major importance when using these RP models to build on surgical guides for implantology (Cillo et al., 2010). SL models have also been used to build surgical guides for zygoma and pterygoid implants in severely atrophied maxillae (Vrielincket al., 2003) and to fix an obturator prosthesis after a large maxillary malignant tumour (Ekstrand & Hirsch, 2008).

2.3.1.3 Stereolithography accuracy

SL models can provide a highly exact reproduction of the skull in children with craniofacial malformations (Frühwald et al., 2008). However, Chang et al. (Chang et al., 2003) found that the mean differences in the overall dimensions between SL models and skull specimens were 1.5 mm (range: 0-5.5 mm) for craniofacial measures, 1.2 mm (range: 0-4.8 mm) for skull base measures, 1.6 mm (range: 0-5.8 mm) for midface measures, 1.9 mm (range: 0-7.9 mm) for maxilla measures, and 1.5 mm (range: 0-5.7 mm) for orbital measures. The mean differences in defect dimensions were found to be 1.9 mm (range: 0.1-5.7 mm) for unilateral maxillectomy, 0.8 mm (range: 0.2-1.5 mm) for bilateral maxillectomy, and 2.5 mm (range: 0.2-7.0 mm) for orbitomaxillectomy defects. Midface SL models may be more prone to error than those for other craniofacial regions because of the presence of thin walls and small projections. Thus, one should consider designing midface bone replacements that are larger in their critical dimensions than those predicted by preoperative modelling. Choi et al. (Choi et al., 2002) found that the absolute mean deviation between an original dry skull and an SL RP model over 16 linear measurements was 0.62 +/- 0.35 mm (0.56+/- 0.39%). These errors were mainly due to the volume-averaging effect, threshold value, and difficulty in the exact replication of landmark locations. Schicho et al. (Schicho et al., 2006) compared the accuracy of CT and SL models. The accuracy for SL models expressed as the arithmetic mean of the relative deviations ranged from 0.8% to 5.4%, with an overall mean deviation of 2.2%. The mean deviations of the investigated anatomical structures ranged from 0.8 mm to 3.2 mm. An overall mean of deviations (comprising all structures) of 2.5 mm was found.

Kragskov et al. (Kragskov et al., 1996) also compared the accuracy of CT and SL models and found that the mean difference over all of the investigated cases was 1.98 mm (3.59%). It should also be noted that the limiting factor in SL model accuracy is the imaging technique, rather than the RP technology used. In general, CT and MRI imaging methods acquire image slices that have a slice thickness on the order of 1.0 to 3.0 mm, which is much greater than the limiting build resolution of any of the RP technologies (Winder & Bibb, 2005). In performing a prospective study on the clinical use of SL models, D'Urso et al. (D'Urso et al., 1999) concluded that SL models significantly improved operative planning and diagnosis. SL models were found to improve measurement accuracy significantly (image measurement error 44.14%, biomodel measurement error 7.91%, $P < .05$). Surgeons estimated that the use of SL models reduced operating time by average of 17.63% and were cost effective with a mean price of $1,031 AUS. Patients found SL models to be helpful in the informed consent process. SL modelling is an intuitive, user-friendly technology that has facilitated diagnosis and operative planning. SL models have allowed surgeons to rehearse procedures readily and improved communication between colleagues and patients. (D'Urso et al., 1999).

2.3.1.4 Stereolithography artefacts

The CT scanning step is important because the quality of the original CT images directly influences the accuracy of a 3D SL model (Choi et al., 2002). The volumetric or 3D image data required for RP models has to follow isotropic multislice CT scanning protocols with a pixel size on the order of 0.5 mm and a slice thickness as low as 1.0 mm (Winder & Bibb, 2005). The CT scanning step can introduce errors in numerous ways, including with respect to section thickness, pitch, gantry tilt, tube current and voltage, patient movement, metal artefacts of intraoral prostheses, and the slice image construction algorithm itself (Choi et al., 2002). Due to the nature of the voxel dimension, the reconstruction of 3D models from CT images involves the interpolation of slices to convert the image data volume into an isotropic dataset set for mathematical modelling (Winder & Bibb, 2005). An inherent problem in this computation is that it smoothes out sharp corners or edges between two slices, which is referred to as the partial volume averaging effect or inter-slice-averaging effect. This effect makes it very difficult to replicate a 3D volume precisely, and because many landmarks are located on sharp vertices or acute edges, the effect may greatly affect the accuracy of 3D models (Choi et al., 2002). The next step consists of the identification and separation of the anatomical structure of interest (segmentation) for modelling from its surrounding structures, which can be performed by image thresholding, manual editing, or autocontouring to extract volumes of interest (Winder & Bibb, 2005). Final delineation of the anatomical structure of interest may require 2D or 3D image editing to remove any unwanted details. A number of software packages are available for data conditioning and image processing for medical RP, including Analyze (Lenexa, KS, www.AnalyzeDirect.com), Mimics by Materialise (Leuven, Belgium, www.materialise.com), and Anatomics (Brisbane, Australia, www.anatomics.net). There remains a need for seamless and inexpensive software that provides a comprehensive range of data interpretation, image processing, and model-building techniques to interface with RP technology (Winder & Bibb, 2005). The size of 3D models depends on the threshold value, which is a specific density in a slice image that separates the organ of interest and other regions. When the threshold value is specified in a slice, it defines contour lines representing the boundary of the organ of interest. The boundaries obtained from every slice form an iso-surface with the same density. Therefore, it is important to select the proper threshold value

(Choi et al., 2002). The first SL models created were for bone, which was easily segmented in CT image data. Bone has a CT number range from approximately 200 to 2,000. This range is unique to bone within the human body, as it does not numerically overlap with any other tissues (Winder & Bibb, 2005). All soft tissues outside the threshold range were deleted, leaving only bone structures. Thresholding required the user to determine the CT number value that represented the edge of bone where it interfaces with soft tissue. The choice of threshold may cause a loss of information in areas where only thin bone is present (Winder & Bibb, 2005). If the bone was particularly thin or the threshold inappropriately measured, a continuous surface was unachievable, leaving the model with a hole where the surface was not closed. In some cases, large areas of bone were removed completely, especially at the back of the orbit and around the malar region (partial volume effect) (Winder & Bibb, 2005). In many circumstances, the volume of the body that is scanned is much larger than that actually required for model construction. To reduce the model size and, therefore the cost, 3D image editing procedures may be employed. The most useful tool for this procedure was a mouse-driven 3D volume editor that enabled the operator to delete or cut out sections from the volume of data. The editing function deleted sections to the full depth of the data volume along the line of sight of the operator. Image editing reduced the overall model size, which also reduced RP building time. Clearer and less complex models may be generated, making structures of interest more clearly visible. Other image processing functions, such as smoothing, volume data mirroring, image addition, and subtraction should be available for the production of models (Winder & Bibb, 2005). When importing data, the key characteristics that determine the size and scale of the data are the pixel size and the slice thickness (Winder & Bibb, 2005). The pixel size is calculated by dividing the field of view by the number of pixels. The field of view is a variable set by the radiographer at the time of scanning (Winder & Bibb, 2005). The number of pixels in the x axis and the y axis is typically 512 x 512 or 1,024 x 1,024. If there is a numerical error in any of these parameters while data are being translated from one data format to another, the model may be inadvertently scaled to an incorrect size (Winder & Bibb, 2005). The slice thickness (Choi et al., 2002) and any interslice gap must be known (although the interslice gap is not applicable in CT imaging, in which images are reconstructed contiguously or overlapping) (Winder & Bibb, 2005). Numerical error in the slice thickness dimension will lead to inadvertent incorrect scaling in the third dimension. This distance is typically on the order of 1.5 mm but may be as small as 0.5 mm or as great as 5 mm. Smaller scan distances result in higher quality of the 3D reconstruction. The use of the internationally recognised DICOM (Digital Image Communications in Medicine) standard for the format of medical images has largely eliminated these errors (Winder & Bibb, 2005). Additional sources of error in 3D model reconstruction include topological defects, such as tessellation, triangle edge, and closure errors, the decimation ratio for surface smoothing, and the methods of interpolation used. The RP manufacturers that provide 3D reconstruction software are concerned with the ability to deal with topological incompleteness and surface smoothness. Errors can arise during the actual production and curing of RP models, including errors associated with the residual polymerisation and transformation of RP materials, the creation and removal of support structures (to avoid unsupported or weakly supported structures), laser diameter, laser path, thickness of layers, and finishing (Choi et al., 2002). Model stair-step artefacts represent the stepped effect seen in medical models. One contribution to these artefacts comes from the discrete layer thickness at which the model is built, which is a characteristic of the particular RP process and material being used. Typically, these thickness range from

0.1 mm to 0.3 mm. This effect can be minimised by selecting processes and parameters that minimise the build layer thickness. However, thinner layers result in longer build- times and increased costs, and an economic compromise is typically found for each RP process. As the layer thickness is typically an order of magnitude smaller than the slice thickness of the CT images, it does not have an overriding effect on the quality of the model. The second effect arises from the slice thickness of the acquired CT or MR images and any potential gap between them (Winder & Bibb, 2005). Both SL and fusion deposing modelling (FDM) required support structures during the build process. These are subsequently cleaned from the model manually, although they generally leave a rough surface, which does not affect the overall accuracy of the model but contributes to a degradation of its aesthetic appearance. It is unlikely that these structures will have a detrimental effect on surgical planning or implant design (Winder & Bibb, 2005). The mathematical modelling of a surface will introduce its own surface effects. The smoothness (governed by the size of the triangle mesh) of the model surface becomes poorer as the surface mesh becomes larger. A larger mesh results in a lower number of triangles, reduced computer file size, and faster rendering. A smaller mesh results in a much better surface representation, much greater computer file size, and slower rendering (Winder & Bibb, 2005).

2.3.1.5 Conclusions

Complex surgical procedures, especially those related to craniofacial structures, appear to benefit significantly from the preplanning and implant construction allowed by physical prototypes. It has been hypothesised that the costs of RP are offset by associated reductions in the number of inaccurate and incomplete complex surgical procedures. The costs of revision procedures and for the replacement of ill-fitting custom implants (which can cost up to $3,000) are significant compared with the cost of applying a centralised rapid medical prototyping service. Many advantages of SL models have been identified: 1) the quality of preoperative planning is greatly improved by allowing a better understanding of the anatomy, and the extent of the disease; 2) the best approach to an osteotomy, and, to the associated surgical site can be assessed, and a more realistic simulation of the surgical steps can be conducted; 3) SL medical models provide an excellent reference when discussing surgical procedures with patients, thus enhancing the validity of informed consent, as the patients gain a greater understanding of the technical difficulties and limitations of the proposed surgery; 4) medical training and surgical education can be undertaken, away from already overcrowded surgical suites, and communication between different specialties allows for a more comprehensive multidisciplinary approach (Cheung et al., 2002); 5) the predicting of results improves with more accurate custom implant manufacturing, preplanned screw placement, and osteotomy design, which also reduces operative time (Arvier et al., 1994; Korves et al., 1995; Murray et al., 2008). SL models can also be sterilised and used directly in the operating theatre. The disadvantages of this technique are mainly those inherent in MRI and CT imaging. Additionally, only one model per simulation can be used, and storage areas will be needed with intense use of these biomodels (Lo & Chen, 2003). Furthermore, the necessary equipment for producing these models is quite costly, and the cost of the fabrication of a composite skull model is presently and is likely to remain very expensive. Although the use of SL models in routine cases is quite rare, they are already in use at various universities and institutions with very satisfactory results, especially in severe cases of maxillofacial deformities (Papadopoulos et al., 2002). Finally, the limitations of the SL modelling technique include a lengthy production time which

renders it unsuitable for emergency cases, and radiation exposure of the patient. With wider use and further technological development, these drawbacks will be minimised. In the future, 3D SL biomodels may become an adjunct not only to maxillofacial surgery but also to other medical specialties (Yau et al., 1995).

2.3.2 Stereolithography Selective Laser sintering (SLS)

2.3.2.1 SLS technique

The SLS technique uses a CO_2 laser beam to selectively fabricate models in consecutive layers. First, the laser beam scans over a thin layer of powder previously deposited on the build tray and levelled with a roller. The laser beam heats the powder particles and fuses them to form a solid layer, and then moves along the *X* and *Y* axes to design the structures according to computer-aided design (CAD) data. After the first layer fuses, the build tray moves downward, and a new layer of powder is deposited and sintered, and the process is repeated until the object is completed. When the manufacturing process is complete, the prototype is removed from the tray, and the surrounding unsintered powder is dusted off. The prototype surface is finished by sandblasting. The SLS prototype is opaque, and its surface is abrasive and porous. Prototype fabrication time is 15 h, and its approximate cost is 600 USD (Sannomiya et al., 2008; Silva et al., 2008). SLS models do not require support structures and are, therefore, relatively easily cleaned, thus saving labour costs (Winder & Bibb, 2005). This technique has been used in the field of craniofacial surgery, reconstructive surgery, orthognathic surgery, pre–prosthetic surgery, tumour surgery, and dental implants.

2.3.2.2 SLS clinical applications

SLS model has been used in the presurgical planning for a tumour surgery (ameloblastoma) to assist with mandibular reconstruction using fibular grafts after ameloblastoma resection. Before surgery, the surgeon used the initial SLS biomodel with the tumour to mark the areas where osteotomies should be performed and to determine the shape and magnitude of an autogenous graft implant. An SLS model could also be used during surgery as a guide for the surgeon to mark the bone graft taken from the fibula and transfer the position of osteotomies from the SLS preoperative model to the operating theatre (Sannomiya et al., 2008). A custom-made SLS model has also been developed that can be fitted at any site of a microvascular fibula flap, taking into account the vascular anatomy (Leiggener et al., 2009). This procedure enhanced the visualisation of points to be remodelled in an autogenous fibular graft to reproduce a new mandible (Sannomiya et al., 2008). The accuracy of SLS model is relatively high with standard errors of a maximum of 0.1 to 0.6 mm. This accuracy depends on the thickness of the CT scans used, which should be as thin as possible (1 to 2 mm is a good compromise for a skull study); the field of view should have a resolution of 512 x 512 and not generate tilting during image acquisition (Leiggener et al., 2009).

Relying on the accuracy of the guide, osteotomies and plating can be safely and swiftly performed with the osseous flap in place, which reduces the ischaemic time. Having access to a virtual plan preoperatively allows a surgical team to discuss a procedure in detail, and surgeons can improve or refine treatment plans and produce custom-made devices in advance. Such virtual plans allow for the movement of bony segments to find the best positions with regard to function, aesthetics and blood supply (the vascular anatomy can be visualised), which means that the optimal donor location on the fibula can be determined. Using RP model to manufacture a guide directly from a dataset obtained from the virtual

plan eliminates the intermediate steps of model construction, from which different types of guides are produced (Leiggener et al., 2009).

A 3D SLS skull model has been found to be able to accurately reproduce and reconstruct a fracture model (Aung et al, 1999) and fully reveal the anatomical structure of the craniomaxillary bone and its relationship to surrounding tissues. It has been used to mimic surgeries for repairing craniomaxillofacial trauma, to determine the validity of a surgical design, to predict surgical outcomes, to weigh various approaches to determine an intraoperative guiding template, and to shorten operation time and minimise surgical risks (Li et al., 2009). The advantage of SLS technology over SL is that it produces models with higher accuracy. This accuracy is especially important in reproducing thin osseous structures of fractured orbital floors for the purpose of manufacturing new custom-made titanium orbital floors (Williams & Revington, 2010). An SLS polyamide model has been used for repairing large skull defects by constructing custom-made cranial plates. Custom-made cranioplasty implants are associated with the advantages of reduced operative time, less invasive surgery, improved cosmetic results, faster recuperation, and reduced costs due to short operative times (Rotaru et al., 2006). SLS models have also allowed for the analysis of abnormalities regarding calvaria morphology, nasal bones and maxilla, improving the criteria for diagnosis and the surgical plan in a case of craniofacial dysostosis (Apert syndrome) (da Rosa et al., 2004; Sannomiya et al., 2006).

2.3.2.3 SLS accuracy

The accuracy of the SLS model is relatively high, with maximum standard errors of 0.1 to 0.6 mm. This accuracy depends on the thickness of the CT scans used, which should be as thin as possible (1 to 2 mm is a good compromise for a skull study); the field of view should have a resolution of 512 x 512 and not generate tilting during image acquisition (Sannomiya et al., 2008). Silva et al. (Silva et al., 2008) and Ibrahim et al. (Ibrahim et al., 2009) found a dimensional error of 2.10% for the SLS prototype in comparison with the dry skull. The authors found an inverse correlation between the external and internal dimensions that may be explained by the dumb-bell effect described by Choi et al. (Choi et al., 2002), in which an increase in external dimensions and a simultaneous decrease in internal dimensions indicated that the prototypes had larger dimensions than the original skull and that the selected threshold may have been too low. Therefore, accuracy is dependent primarily on the choice of scanning protocol, on data segmentation and, especially, on the determination of the threshold. One factor that may partially explain the smaller dimensions of SLS prototypes is the superficial wear caused by sandblasting (Silva et al., 2008). The unused powder that surrounds the prototype in the SLS system cannot be reused. Because of the high cost of the material, several parts are fabricated simultaneously. The long fabrication time for the SLS technique (16 h) is very close to the time required for fabrication with the SL system (Silva et al., 2008).

2.3.3 Fused deposition modelling (FDM)

2.3.3.1 FDM technique

Fused deposition modelling (FDM) uses a similar principle as SL in that it builds models on a layer-by-layer basis. The main difference is that the layers are deposited as a thermoplastic that is extruded from a fine nozzle. A commonly used material for this procedure is acrylonitrile butadiene styrene (ABS). The physical properties of ABS are that it is rigid, has

dimensional stability, exhibits thermoplastic properties, and is inexpensive. The 3D model is constructed by extruding the heated thermoplastic material onto a foam surface in a path guided by the model data. Once a layer has been deposited, the nozzle is raised between 0.178 to 0.356 mm, and the next layer is deposited on top of the previous layer. This process is repeated until the model is complete. As with SL, support structures are required for FDM models, as it takes time for the thermoplastic to harden and the layers to bond together. The supports are added to the model at the design stage and are built using a different thermoplastic material, which is extruded through a second nozzle. The support material is of different colour than the building material and does not adhere to it, which enables the easy identification and subsequent removal of the supports by hand after the model is completed. A recent development related to this technique is the availability of a soluble support material, which enables support structures to be dissolved from the model in an agitated water bath (Winder & Bibb, 2005). In this systematic review, we found that only a surgical template for dental implant drilling had thus far been developed based on this technique (Sohmura et al., 2009).

2.3.4 3D Printing (3DP)

2.3.4.1 3DP technique

The 3D printing (3DP) system uses print heads to selectively disperse a binder onto powder layers. This technology has a lower cost than similar techniques. First, a thin layer of powder is spread over a tray using a roller similar to the one used in the SLS system. The print head scans the powder tray and delivers continuous jets of a solution that binds the powder particles (gypsum powder with a lateral resolution of 200 μm or less) as it touches them. No support structures are required while the prototype is fabricated because the surrounding powder supports the unconnected parts. When the process is complete, the surrounding powder is aspirated. In the finishing process, the prototype surfaces are infiltrated with a cyanoacrylate-based material to harden the structure (Silva et al., 2008). The printing technique enables the formation of complex geometrical structures, e.g., hanging partitions inside cavities, without artificial support structures. After the CT scan the rendering of the DICOM data and transformation into STL takes a maximum of a half an hour, and the printing process and infiltration takes approximately 4-6 h. The material costs for the construction of each model are € 150–200 each (Silva et al., 2008; Klammert et al., 2009). The 3D printers used in this process are relatively inexpensive (£25,000), have fast build times (4 h for a full skull), and are easy to maintain. Additionally, 3D printers are cost effective (£1/cm^3), associated with low waste, accurate (±0.1 mm in the *Z* plane, ±0.2 mm in the *X*, *Y* planes), have small dimensions and can make hard, soft or flexible models. These printers can also be used to identify different types of body tissue depending on the predefined threshold setting selected (Aleid et al., 2010).

2.3.4.2 3DP clinical applications

The reduction of fractures in 3DP models of the maxillofacial region before surgery provides a number of advantages. The most important of these is the global perspective of the reconstruction that the 3D model provides. The widths of the maxillary and mandibular arches and the symmetry of the reconstruction can be easily evaluated in 3 dimensions using this technique. Additionally, planning for certain types of surgery, particularly the repair of discontinuity defects of the mandible, is greatly improved by the ability to evaluate the

alignment of mandibular segments based on mirror imaging of the contralateral side, which greatly enhances the accuracy of the reconstruction. Of course, there is an effort investment required in preparing the model. The task of converting CT images using interactive segmentation software and the generation of the model can be managed by technical staff. However, the surgery on the RP model and the reduction of fractures both require the skills of a surgeon (Aleid et al., 2010). It is important to emphasise the fact that reconstruction plates contoured before surgery act as templates to ensure the accuracy of the reconstruction. When plates contoured on 3D models before surgery are used, they bring the segments into alignment when they are fixed to the bone with screws. Therefore, the contoured plates not only serve to reconstruct the fracture but also act as templates to establish the final phase of alignment with precision (Wagner et al., 2004). A 3DP model has also been used for repairing orbital floor fractures using pre-shaped titanium mesh implants formed based on anatomical 3DP models of the orbit (Kozakiewicz et al., 2009). The unaffected orbit was mirrored onto the contralateral side, i.e., the injured orbit. This model contained numerous artefacts, which is typical of CT studies because of the very thin bone structures of the orbit. To create a rigid physical model that will be strong enough to be used as a template, all of the empty spaces (air) surrounding the mirrored orbit in the virtual model were filled in, which resulted in a virtual model of the orbit that was surrounded only by hard tissue. Next, the virtual model data were converted to an STL format, and solid physical models were created from acrylic resin using a 3D printer. The resulting physical models were stronger and more rigid than if they had been built containing hollow structures i.e., maxillary and ethmoid sinuses (Kozakiewicz et al., 2009). The use of 3DP models in orbital floor reconstruction has numerous advantages, such as the following: 1) increasing the understanding of orbital disruption; 2) shortening the operation time; 3) decreasing the number of attempts at positioning an implant in the orbit and verifying the shape and fit; 4) serving as a guide for the surgeon during an operation; 5) being relatively inexpensive. However, this method is also associated with some disadvantages, such as the following: 1) the length of time required to build model; 2) the cooperation required between a number of people in different locations; and 3) the use of this method in panfacial fractures is challenging because it is difficult to find any stable orbital margins for virtual planning of the model and to establish an accurate position for the pre-shaped plates (Kozakiewicz et al., 2009).

Preoperative orthognathic surgery plans can be tested using 3DP models. The relationship between proximal and distal mandibular segments after bilateral sagittal split osteotomies has been evaluated on models preoperatively. Studying the planned movements of osteotomised bone segments preoperatively and observing the relationships of osteotomised segments of the mandibula and maxilla in orthognathic surgery increased the intraoperative accuracy (Mavili et al., 2007). A 3DP multi-position model was also used to prebend titanium plates and produce a surgical guide for transferring osteotomies from the 3DP model to the operating theatre in genioplasty (Olszewski et al., 2010).

Additionally, 3DP models have been used for planning distraction osteogenesis related to complex craniofacial malformations (osteotomies, vector of distraction). The customised fixation plates of a distractor primarily prepared based on the 3DP model can be easily adapted during surgery to predicted positions due to their high accuracy of fit, and they enable the parallel alignment of both connecting pins, which ensures the proper transmission of distraction forces to the mobilised segment (Klammert et al., 2009).

Furthermore, 3DP models have been used in mandibular resection (Ortakoglu et al., 2007) and reconstruction using a reconstructive plate. The plate was precontoured according to

the 3DP model. Precise adaptation of the plate and excellent symmetry were achieved within a relatively short operation time. Plate handling in the operating theatre was minimal, thus preserving its strength. Other benefits of using 3DP models include decreased exposure time to general anaesthesia, decreased blood loss and shorter wound exposure time. The advantages of 3DP model techniques include the special understanding of bone morphology that is provided, accurate and easier planning of preoperative plate bending, and much more accurate bone harvesting due to using the negative imprint of the gap to be reconstructed. Thus, 3DP technology is a reliable method for assisting in precise mandibular reconstruction using bone plates and bone grafts. Compared with other 3D methods, this method can be performed more quickly and easily and is more cost effective. Furthermore, it is superior in printing smaller and more complex structures (Cohen et al., 2009).

2.3.4.3 3DP accuracy

Silva et al. (Silva et al, 2008) reported a mean dimensional error of 2.67% in prototypes produced using 3DP technologies in comparison with a dry human skull (criterion standard). In the 3DP system, the printing mechanism, the type and quality of the materials used in the fabrication of the prototypes, and the absorption properties of the powder when in contact with the binder and infiltration material are parameters that should be controlled to obtain a reliable final product. It is possible that the 3DP prototypes were larger than the dry skulls because of cyanoacrylate infiltration. The powder remaining in the 3DP system may be reused, and the parts may be fabricated individually, which substantially reduces prototype fabrication time (4 h). Therefore, the 3DP technique has a lower final cost than the SLS technique, which, in turn, has a lower cost than the SL technique (Silva et al., 2008). Advantages of 3DP over SLS include a faster printing time and lower costs (Cohen et al., 2009). However, SLS prototypes have a better dimensional precision and reproduce anatomical details of the craniomaxillary region more accurately than 3DP prototypes (Silva et al., 2008). Ibrahim et al. obtained a dimensional error for 3DP of 1.07 mm (2.67%) when comparing SLS (0.89 mm and 2.10%) and 3DP models and dry skulls (Ibrahim et al., 2009).

2.3.5 Polyjet modelling

Polyjet modelling is performed by jetting state-of-the-art photopolymer materials in ultra-thin layers (16 μm) onto a build tray layer by layer until the model is completed. Each photopolymer layer is cured by UV light immediately after it is jetted, producing fully cured models that can be handled and used immediately, without post-curing. The gel-like support material used, which is specially designed to support complicated geometries, is easily removed by hand and water jetting. At present, this technique is too time- consuming and, therefore, too expensive to be used in CMF surgery clinical applications. Ibrahim et al. (Ibrahim et al., 2009) reported a dimensional error of 2.14% in reproducing a dry mandible when using this technique.

3. Clinical examples of applications of use of RP models in CMF surgery

3.1 Three-dimensional rapid prototyping model, modeling clay, surgical guide, and pre-bent titanium mesh in reconstruction of the posttraumatic orbital floor

3.1.1 Introduction

Different methods, surgical approaches, and materials (Schon et al., 2006; Kozakiewicz et al., 2009) were proposed for reconstruction of the posttraumatic orbital floor. Recently, the use

of three-dimensional (3D) pre-bent titanium implants in a 3D rapid prototyping (3D RP) model was introduced (Kozakiewicz et al., 2009). However, even if the pre-bent titanium mesh fits perfectly on the 3D RP model, transfer of the pre-bent mesh from the 3D RP model to the operating room while maintaining exact an position remains challenging. Therefore, we present a method that involves the use of a rapid prototyping model-based prefabricated surgical drill guide to improve the pre-bent titanium mesh positioning.

3.1.2 Case report

A 38-year-old male patient presented to our Department of Oral and Maxillofacial Surgery three weeks after facial trauma incurred during his weekly boxing course. Anamnesis revealed a period of extensive left periorbital swelling immediately following the injury. However, no medical consultation was performed at that time. The clinical examination revealed a left eye enophtalmos and an upgaze diplopia. The patient also presented a hypoesthesia of the left infra-orbital nerve. The patient's main concern was esthetic, related to the accentuated palpebral fold on the left side. A low-dose CT scan was performed (Olszewski et al., 2008). The patient presented with a combined maxillofacial fracture of the left orbital floor, the left anterior maxillary sinus wall and the nasal bones (Fig 1A, C).

3.1.3 Method

A 3D RP model (Z Corp, Burlington, USA) was created based on low-dose CT data (DICOM files, STL format) (Olszewski et al., 2008). We used modeling clay (Décor fin, Royal Talens, Holland) to fill in all the holes of the orbital floor on the 3D RP model. The modeling clay also served to reconstruct the left orbital floor such that it was symmetric to the right side. Then, a sheet of paper was cut to fit in the left orbital floor. A titanium mesh (0.4 -mm in width) was then cut from a 100 x 100 -mm titanium mesh plate (Synthes, Oberdorf, Switzerland) with a sheet of paper as a guide. The titanium mesh was then applied and pre-bent on the 3D RP model. The holes for the screws were marked with a pencil on the anterior orbital rim of the 3D RP model (Fig 2 A). The acrylic guide for positioning the screws was prepared according to the shape of the left orbital rim. Aluminum cylinders were inserted into the acrylic surgical guide to guide the 1.8 -mm diameter drill. The aluminum cylinders were inserted perpendicular to the underlying bone surface (Fig 2 B). The pre-bent titanium mesh and the acrylic guide were sterilized using a standard procedure. The fracture site was exposed with the patient under general anesthesia, via a subciliary approach to the left orbital floor. The herniated fat and muscle tissue were moved up to avoid further necrosis and to increase the intra-orbital volume. The prefabricated surgical acrylic guide was inserted in the inferior left orbital rim (Fig 2 C). Four holes were drilled in the left orbital rim, through the guide, using an 8 -mm drill. The pre-bent titanium mesh was then positioned in the orbit and fixed to the inferior orbital rim by means of three 4 -mm screws and one 6 -mm screw. The diameter of each screw was 1.8 -mm (Fig 2 D). Clinical postoperative follow-ups at one week and one month showed no diplopia and correction of the palpebral fold. Radiological follow-up revealed a restitutio ad integrum of the left orbital floor (Fig. 1 B, D).

3.1.4 Discussion

The recently presented use of pre-bent titanium mesh in 3D RP models (Kozakiewicz et al., 2009; Scolozzi et al., 2009) allows for accurate repositioning of a de novo reconstructed

orbital floor. However, there are multiple alternative positions for insertion and positioning of the pre-bent titanium mesh inside the orbit. This is especially true for medio-lateral positioning of the titanium mesh, due to relative lack of precise anatomical landmarks on the inferior orbital rim. The acrylic surgical guide allows for transfer of holes for screws from the position appropriate for 3D RP planning to that used in the operating theater (Olszewski et al., 2010). Therefore, there exists only one three-dimensional position for the pre-bent titanium mesh inside the orbit. This cost-effective method could also be an alternative to most cost- and time- consuming navigation-based methods (Ewers et al., 2005; Bell & Markiewicz, 2009). To pre-bend the intra-orbital part of the titanium mesh a 3D virtual model of the orbit was described and constructed as a 3D RP model (Kozakiewicz et al., 2009). The 3D virtual model required two steps: 1) a mirroring of the right side of the orbital floor on the left side and, 2) a virtual filling in all the empty virtual spaces present because of partial volume effect and of true spaces, that are anatomically present. All these steps were time-consuming and necessitated an experienced engineering team (Kozakiewicz et al., 2009). Use of the modeling clay directly on the 3D RP model precludes the need for time-consuming, complex computer-assisted manipulations, knowledge of advanced software, or an engineering team. Finally, the use of a sheet of paper allows economical use of 100 x 100 -mm mesh titanium plates.

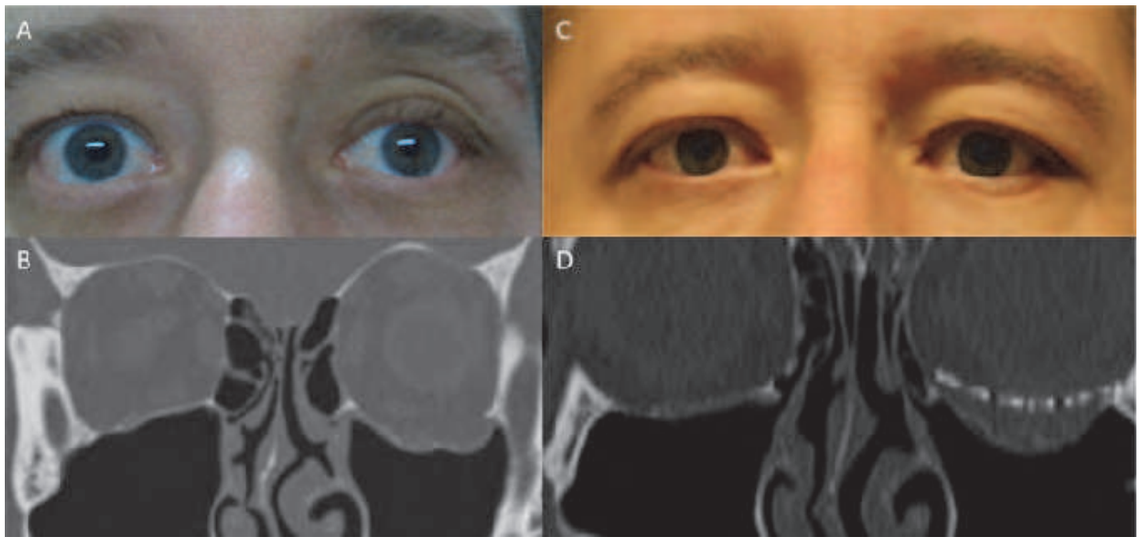

Fig. 1. (A) Pre-operative appearance of the face, accentuated palpebral fold on the left side; (B) Preoperative low-dose CT scan, coronal view; (C) Postoperative appearance of the face, correction of the upper left palpebral fold; (D) Postoperative low-dose CT scan, coronal view, restoratio ad integrum of the inferior orbital wall with the preshaped titanium mesh.

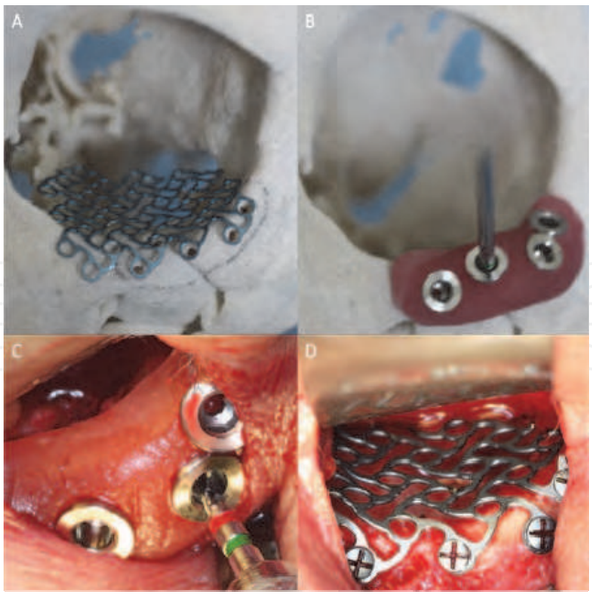

Fig. 2. (A) Pre-bent titanium mesh on the three-dimensional rapid prototyping (3D RP) model, with holes for screws and size of the guide marked with black pencil on the 3D RP model; (B) Acrylic surgical guide for positioning the holes for screws on the 3D RP model, positioning of the drill at 90° in relation to the bone surface; (C) Intra-operative drilling of holes through the surgical guide; (D) Intra-operative view of the positioning of the pre-bent titanium mesh on the left orbital floor.

3.2 Innovative procedure for computer-assisted genioplasty: three-dimensional cephalometry, rapid prototyping model and surgical splint.

3.2.1 Introduction

Genioplasty plays an important role in harmonizing facial proportions and profiles. However, planning a genioplasty remains a difficult task because of limited means of diagnosis, planning and information transfer to the operating room (OR). Specifically, the theoretical virtual anteroposterior and vertical positions of the chin are reduced to the landmarks "menton", "B point", and "pogonion" on two-dimensional cephalograms (Ayoub et al., 1994). We propose and describe the combined use of three-dimensional (3D) cephalometry, a 3D rapid prototyping model, and pre-bent titanium plates as a new means of computer-assisted genioplasty.

3.2.2 Method

A young adult patient presented in our clinics after an orthodontic treatment was completed elsewhere. At clinical examination, the patient still presented a retrusive profile and refused any orthognathic treatment for the occlusion (Figure 3A). Therefore, we proposed an advancement genioplasty. We received approval from the local ethics committee (B40320084307) for the clinical application of the 3D cephalometric analysis, and the subject gave informed consent for the study. A low-dose CT scan of the head was performed (Olszewski et al., 2008) from which we determined the anterior, posterior, and inferior limits of the chin with the newly-developed and validated 3D cephalometric planar analysis (ACRO 3D) (Figure 3B) (Olszewski, 2007, 2008). The osteotomy lines were

planned and visualized with Mimics software (Materialize, Leuven, Belgium). We positioned the upper osteotomy line at a distance of at least 5 mm from both mental foramina. The amount of movement was virtually planned with Mimics software in relation to the reference planes from the ACRO 3D analysis (Figure 3B). We then built a 3D rapid-prototyping model (RPM) from the low-dose CT scan with a 3D printer (Z-Corp, Burlington, USA) (Silva et al., 2008). The 3D RPM was presented as a multi-position 3D model (Figure 4) with initial, intermediary, and final positions of the bony slices of the chin. We used the final position of the 3D RPM to pre-bend the titanium plates and to indicate the positions of the holes for screws corresponding to the pre-bent plates. The 3D RPM model was then repositioned to its initial position and an acrylic surgical guide was made. The role of the surgical guide was to transfer the position of the holes for the screws (in their final position) and the osteotomy lines. The surgical guide was sterilized at 120° Celcius for 20 minutes in an autoclave. The pre-bent titanium plates were also sterilized (Kozakiewicz et al., 2009). During the surgery and before the osteotomy, the acrylic guide was positioned on the osseous chin of the patient. First, we drilled the holes for the screws through the surgical guide (Figure 5). Then, with a sterilized pencil (Husami et al., 1988) we drew the osteotomy lines based upon the surgical guide (Figure 5). Osteotomy cuts were performed following the pencil tracings. Finally, after complete separation of the bony fragments, we positioned and screwed the pre-bent plates (Figure 6). A low-dose CT scan showed a good result in the patient's profile (Figure 3, C).

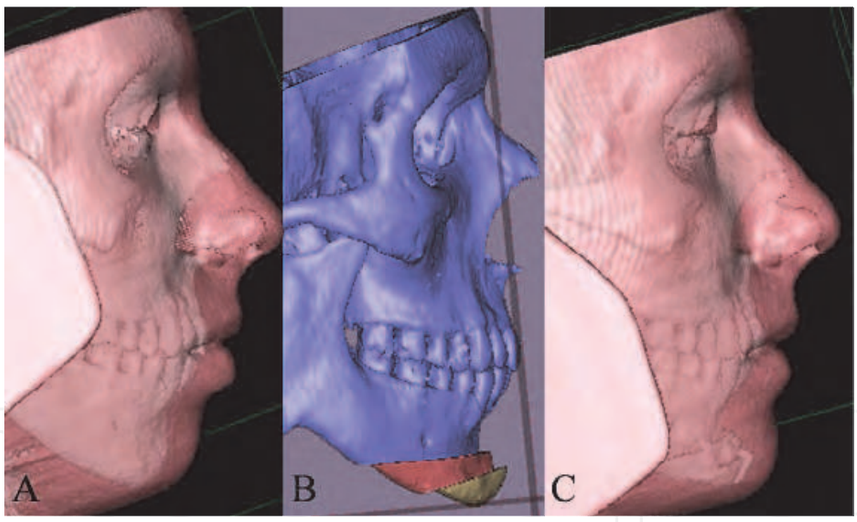

Fig. 3. A. Pre-operative profile; B. Virtual planning, double advancement of the chin; C. Post-operative profile.

3.2.3 Discussion

Computer-assisted genioplasty seems to be the next step in the evolution of computer-assisted orthognathic surgery (Xia et al., 2000). The combination of different three-dimensional methods for the diagnosis (3D cephalometric analysis), virtual planning (Mimics software), and transfer (3D RPM, surgical guide, and pre-bent plates) allowed for a complete 3D treatment of this case. The 3D cephalometry plays an important role in planning a genioplasty. For the first time, the chin region was evaluated with more than a

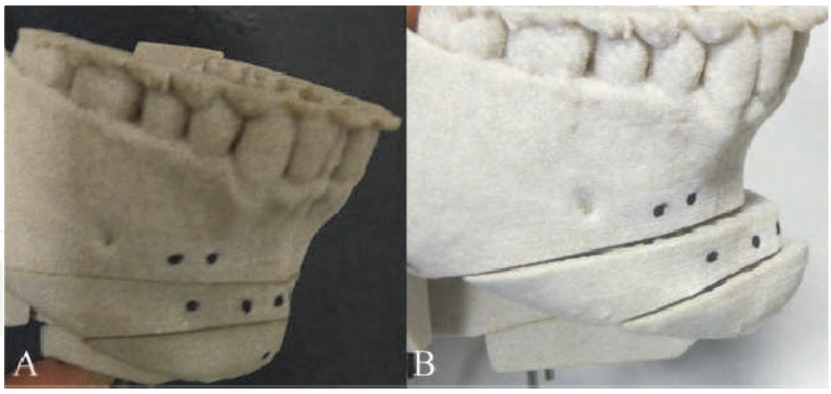

Fig. 4. A. Pre-operative initial position. B. Postoperative final position. Black dots indicate the position of holes for the screws.

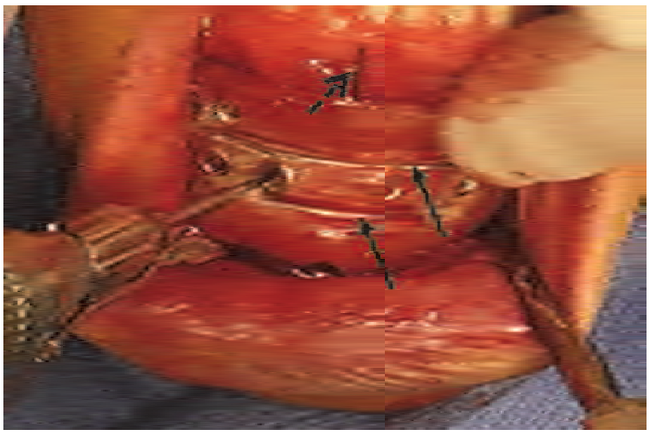

Fig. 5. Acrylic guide positioned on the osseous chin of the patient. Holes for the screws drilled through the surgical guide. Plain arrows showing transfer lines for osteotmy paths. Discontinoous arrow shows the midline indicator of the acrylic guide.

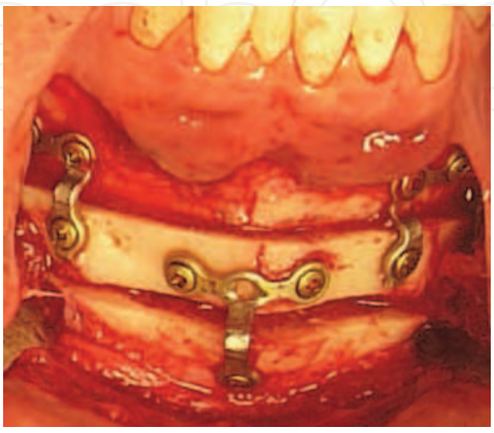

Fig. 6. Positioning and screwing of the pre-bent plates.

single landmark ("menton", or "pogonion") as is normally the case with 2D cephalometrics (Ayoub et al., 1994). We have limited the presentation of the 3D cephalometry in Figure 3 to the region of interest, which was the evaluation of the chin. The concept, software, and experimental validation of the 3D cephalometric planar analysis have been previously published (Olszewski et al., 2007). Three planes (anterior, posterior and inferior) determine the theoretically ideal and individual position for the osseous chin volume in the 3D space. However, the final decision for the position of the chin must also involve consideration of the soft tissue in the patient's profile. The position of the chin is dependent on the desires of the patient and on the clinical judgment of the surgeon. Therefore, there can be a discrepancy between the conclusions of the theoretical 3D cephalometry and the clinical experience. In this case, the final amount of bone movement in the anteroposterior direction was inferior to that proposed by the 3D cephalometric analysis (anterior plane). It must be stressed that the visualization of soft tissues in figures 3A (preoperative) and 3C (postoperative) represents the true soft-tissue profile of the patient pre- and post-operatively. Virtual planning showed that there was only a place for one screw on the lower part of the chin osteotomy. With the virtual planning we decided preoperatively on the best positioning for that screw. The stability of the lower part of chin osteotomy was also achieved with a pre-bent plate formed on the 3D rapid model. Virtual planning allows for the visualization of the roots and for better positioning of the screws in relation to the roots. For that reason, the chance of root damage is very low in comparison to techniques without a computer-generated surgical splint. The 3D RP model allowed for a transfer of parallel osteotomy lines to the OR. We also were able to propose a sandwich technique, which allowed for the following: 1) a bigger advancement compared to one-piece movement, and 2) improved stability and healing of the displaced bony slices. The use of the sterilized computer-generated surgical guide and pencil was also cost-effective compared to currently available navigation systems (Ewers et al., 2005). We modified the use of the 3D RPM from a diagnosis-only purpose (Santler et al., 1998) to making a transfer of virtual information to the OR. It should be stressed that building a 3D RPM with 3D printers is now more affordable (less than 300 Euros for a 3D RP model) than stereolithographic models (Kozakiewicz et al., 2009). Also, the time spent on the osteotomy and on bending plates was decreased during surgery. The possible chin drop related to increased muscle detachment in the sandwich technique was avoided due to mental muscle reattachment at the end of the surgery. The postoperative results of the new technique are promising. The technique is fast and is easy-to-use due to its computer-generated surgical splint and pre-bent plates. More patients are needed for definitive clinical validation of this procedure. Of note, the same approach of combining 3D cephalometric analysis, 3D multi-position RPMs, surgical cost-effective computer-generated surgical guides and pre-bent plates may be of interest in other orthognathic surgery.

3.3 New three-dimensional (3D) surgical guide for frontal-nasal-ethmoid-vomer osteotomy

3.3.1 Introduction

Lefort III surgery is a classical surgery performed to correct craniofacial craniosynostoses (Epker &Wolford, 1980). The majority of the osteotomy lines are performed through via open sky access or with the tactile contact (pterygopalatine disjunction with an Obwegeser osteotome). However, frontal-nasal-ethmoid-vomer osteotomy is performed in a blind manner based only on the experience of the surgeon. The main risks during this type of

osteotomy are linked to the initial wrong three-dimensional orientation of the osteotome in relation to the patient's anatomy. The anatomy of a craniosynostotic syndromic patient could also be misleading for initial orientation of the osteotom (Sannomiya et al., 2006). An osteotomy performed in too anterior and/or too lateral a direction could result in a bad split of the midline during the down-fracture with Rowe forceps. If performed in too posterior a direction, the ethmoid body could be entered, resulting in intense bleeding and olfactive nerve damage. Finally the depth of insertion of the osteotome in relation to the frontonasal suture is also an issue: too short an insertion will result in incomplete midfacial disjunction and uncontrolled midfacial fracture during the down-fracture with Rowe forceps. Therefore, we propose a new technique based on a three-dimensional (3D) surgical guide for frontal-nasal-ethmoid-vomer osteotomy based on a 3D rapid prototyping model. The method was applied to a 7- year- old Apert craniosynostosis patient. Lefort III osteotomies were associated with internal distraction devices for the midface advancement (Nout et al;, 2008).

3.3.2 Material and methods

A three-dimensional (3D) computed tomography (CT) of the skull was acquired in a standard head position with a previously validated low- dose CT protocol (Olszewski et al., 2008) (Brilliance 64, Philips, Eindhoven, the Netherlands). The protocol dictates a 1mm slice, with 512x512 matrix, 210 mm field of view, 120 kV and 42 mA. The native data were saved on a CD (DICOM format). The 3D CT reconstruction was performed by Mimics software (Materialize, Leuven, Belgium) and saved under STL format. A rapid prototyping (RP) model of the skull was obtained with a 3D printer (Z Corp, Burlington, USA). We drilled a groove in the nasal bones until the frontal-nasal suture was reached. A osteotome of 5 mm width was positioned inside the nasal fossa, with anterior-posterior orientation, from the nasal-frontal suture toward the level of posterior nasal spine. Following this, PMMA resin (Palacos, Heraeus Medical, Germany) was moulded around the osteotome and around the nasal bones (Figures 7,8).

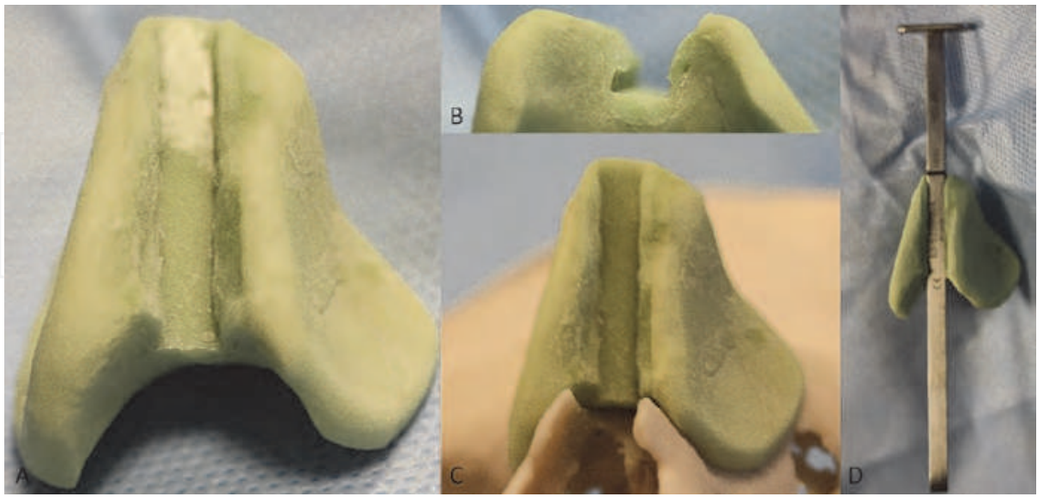

Fig. 7. A. Anterior view of customized 3D osteotomy guide in PMMA resin . B. Inferior view of the 3D guide: the groove for osteotome. C. Anterior view: positioning of the 3D guide on the 3D RP model. D. Anterior view: checking the sliding movement of the osteotome through the 3D guide. The final depth to insert the osteotome is indicated with alcohol pen.

After the thermo-reaction ended, the 3D guide was polished with dental burrs and sterilised in an autoclave under standard conditions (135°C, 20 minutes). The distance from the top of the 3D guide and the posterior nasal spine was also measured on the 3D RP model (8.3 cm).

Fig. 8. A. Positioning of the 3D guide, and osteotome on the patient's 3D RP skull model. B. Superior view: checking the insertion of the osteotome inside the 3D guide. C. Inferior view: checking the posterior limit of the osteotomy at the level of posterior nasal spine.

Fig. 9. A. Intra-operative view. Insertion of the osteotome with the 3D guide trough the nasal bones (dashed arrow) until reaching the predicted depth (arrow shows a mark on osteotom). On the right, orbitofrontal bandeau is deposed at that time of surgery, and compresses cover the brain (*). On the left, bicoronal flap raised up at the beginning of the surgery(**).

3.3.3 Results

The surgery was then performed classically with bi-coronal and intraoral accesses. All Lefort III osteotomies were performed classically with drills and osteotomes. The 3D guide was positioned on the top of the frontal-nasal sutures. No cranial pressure was induced with the 3D guide at any time during the procedure. We used an osteotome of 5 mm width. We

marked a reported distance from the 3D RP model (Figure 8.A) on the osteotome with an alcohol pen (Figure 9, arrow). The osteotome was then positioned in the flat groove inside the 3D guide and inserted into the bone with the orientation provided by the 3D guide until it reached the marked depth (at the level of posterior nasal spine) (Figure 9, arrow).

3.3.4 Discussion

Performing frontal-nasal-ethmoid-vomer osteotomy seems to be one of critical issues in Lefort III surgery (Gosain et al., 2002; Matsumoto et al., 2003). Therefore, every technique facilitating this procedure could immediately help the surgeon and protect the patient from major complications. We presented a technical approach based on the optimisation of the use of 3D RP models. 3D RP models are mainly used for diagnostic purposes (Santler et al., 1998). However, 3D RP models allow also for the transfer of 3D data from planning to the operating theatre (Kozakiewicz et al., 2009). We used a 3D printer technique (Z Corp, Burlington, USA) to build a 3D RP model of the skull (Kozakiewicz et al., 2009). The 3D printed models have an economical advantage over stereolithography and retain the accuracy required for medical modelling (Ibrahim et al., 2009). The PMMA resin (Palacos, Heraeus Medical, Germany) was used to create the 3D guide. This material is easy to use, cost -effective, and allows for fast 3D moulding of the frontal-nasal area. The positioning of the 3D guide on the patient does not require a supplementary task by the surgeon, such as registration and tracking in intra-operative navigation (Jeelani et al., 2009). The individualized 3D guide allows three main pieces of information to be transferred from the 3D RP model: impact point for the osteotome, orientation in the 3D space, and the depth for the insertion of the osteotome. This technique allows a critical osteotomy path in Lefort III surgery to be transferred in a secure, fast, and cost-effective manner from the 3D RP model to the operating room. Further study will consists in verification of the accuracy of using customized 3D guides for subcranial separation of the face at the nasofrontal region on cadavers.

4. Conclusions and future directions

Three-dimensional RP models are used in association with a variety of applications in CMF surgery. However, there is still room for innovation in these models and for new uses related to additional indications. Increasing the accuracy of RP techniques is still required but without supplementary irradiation of the patient. For this reason, attention should focus on the implementation of low-dose CT scans and cone beam CT scan protocols for data acquisition. Additionally, an effort should be made to develop 3D RP models from alternative image sources, such as MRI, ultrasounds, and laser scan imaging. More cost-effective methods are required for the broad application of these modeling technique beyond the most developed countries. For this reason, 3DP currently appears be more realistic for current clinical use than SL or SLS techniques. Other cost-effective RP techniques, such as 3D paper printing (http://www.mcortechnologies.com), should also be investigated in terms of accuracy and applicability and, to increase the availability of 3D RP technology to CMF surgeons and to improve patient care. Such 3D RP models should be used not only for diagnostic purposes but also mainly for transferring virtual plans to the operating theatre. In this process, 3D RP models will be competitive against computer-assisted navigation techniques, which are accurate but still very expensive and time-consuming. Another important factor related to the use of these models is the time required

for their fabrication, which should be shortened to allow the use 3D RP techniques directly in emergency rooms to enlarge the field of potential indications they may be used to adress. There is still a need for the development of guidelines for 3D RP models related to their clinical use in CMF surgery for the purpose of determining which technique (with which protocol) is best for addressing each specific indication. Finally, CMF surgery will certainly profit from the most advanced and emerging 3D printing techniques, such as organ printing (Song et al., 2010). Organ printing is a biomedically relevant variant of rapid prototyping technology, which is based on tissue fluidity. Computer-assisted deposition (printing) of natural materials (cells or matrices) is performed one layer at a time until a particular 3D form is achieved (Jakab et al., 2010). However, recent attempts using rapid prototyping technologies to design solid synthetic scaffolds (Song et al., 2010) suffered from an inability to precisely place cells or cell aggregates into a printed scaffold. Thus, organ-printing technology will become increasingly more *secondum naturam*. Mironov et al., (Mironov et al., 2003, 2011) defined organ printing as a rapid prototyping computer-aided 3D printing technology based on using the layer-by-layer deposition of cells and/or cell aggregates into a 3D gel, with the subsequent maturation of the printed construct in perfused and vascularised living tissues or organs. This definition of organ printing includes the many different printer designs and components associated with the deposition process that are currently available, such as jet-based cell printers, cell dispensers or bioplotters, different types of 3D hydrogels and varying cell types. Such computer-assisted tissue engineering using 3D live RP technology will certainly open a new era for reconstructive CMF surgery.

5. References

Al-Ani SA, Locke MB, Rees M & de Chalain TM. (2008). Our experiences managing a rare cranio-orbital cleft. *J Craniofac Surg*, 19, 3, (May 2008), pp. (819-822) ISSN 1049-2275

Aleid W, Watson J, Sidebottom AJ & Hollows P. (2010). Development of in-house rapid manufacturing of three-dimensional models in maxillofacial surgery. *Br J Oral Maxillofac Surg*, 48, 6, (September 2010), pp. (479-481)

Al-Sukhun J, Törnwall J, Lindqvist C, Kontio R & Penttila H. (2008). One-stage zygomaticomandibular approach for improved access to the hemimaxilla and the middle base of the skull. *J Craniofac Surg*, 19, 2, (March 2008), pp. (528-533)

Arnaud E, Marchas D & Renier D. (1997). Aplasia of the vertex without scalp defect. *J Craniofac Surg*, 8, 2, (March 1997), pp. (146-150)

Arvier JF, Barker TM, Yau YY, D'Urso PS, Atkinson RL & McDermant GR. (1994). Maxillofacial biomodelling. *Br J Oral Maxillofac Surg*, 32, 5, (October 1994), pp. (276-283) ISSN 0266-4356

Aung SC, Tan BK, Foo CL & Lee ST. (1999). Selective laser sintering: application of a rapid prototyping method in craniomaxillofacial reconstructive surgery. *Ann Acad Med Singapore*, 28, 5, (September 1999), pp. (739-743) ISSN 0304-4502

Ayoub AF, Stirrups DR & Moos KF. (1994). Assessment of chin surgery by a coordinate free method. *Int J Oral Maxillofac Surg*, 23, 1, (February 1994), pp. (6-10) ISSN 0901-5027

Bell RB & Markiewicz MR. (2009). Computer-assisted planning, stereolithographic modeling, and intraoperative navigation for complex orbital reconstruction: a

descriptive study in a preliminary cohort. *J Oral Maxillofac Surg,* 67, 12, (December 2009), pp. (2559-2570)

Bill JS, Reuther JF, Dittmann W, Kübler N, Meier JL, Pistner H & Wittenberg G. (1995). Stereolithography in oral and maxillofacial operation planning. *Int J Oral Maxillofac Surg*, 24, 1 Pt 2, (February 1995), pp. (98-103) ISSN 0901-5027

Cao D, Yu Z, Chai G, Liu J & Mu X. (2010). Application of EH compound artificial bone material combined with computerized three-dimensional reconstruction in craniomaxillofacial surgery. *J Craniofac Surg*, 21, 2, (March 2010), pp. (440-443)

Chang PS, Parker TH, Patrick CW Jr & Miller MJ. (2003). The accuracy of stereolithography in planning craniofacial bone replacement. *J Craniofac Surg*, 14, 2, (March 2003), pp. (164-170)

Chang SC, Liao YF, Hung LM, Tseng CS, Hsu JH & Chen JK. (1999). Prefabricated implants or grafts with reverse models of three-dimensional mirror-image templates for reconstruction of craniofacial abnormalities. *Plast Reconstr Surg*, 104, 5, (October 1999), pp. (1413-1418)

Cheung LK, Wong MC & Wong LL. (2002). Refinement of facial reconstructive surgery by stereo-model planning. *Ann R Australas Coll Dent Surg*, 16, (October 2002), pp. (129-132)

Choi JY, Choi JH, Kim NK, Kim Y, Lee JK, Kim MK, Lee JH, Kim MJ. (2002). Analysis of errors in medical rapid prototyping models. *Int J Oral Maxillofac Surg*, 31, 1, (February 2002), pp. (23-32) ISSN 0901-5027

Cillo JE Jr, Theodotou N, Samuels M & Krajekian J. (2010). The tent pole splint: a bone-supported stereolithographic surgical splint for the soft tissue matrix expansion graft procedure. *J Oral Maxillofac Surg*, 68, 6, (June 2010), pp. (1365-1370)

Cohen A, Laviv A, Berman P, Nashef R & Abu-Tair J. (2009). Mandibular reconstruction using stereolithographic 3-dimensional printing modeling technology. *Oral Surg Oral Med Oral Pathol Oral Radiol Endod*, 108, 5, (November 2009), pp. (661-666)

da Rosa EL, Oleskovicz CF & Aragão BN. (2004). Rapid prototyping in maxillofacial surgery and traumatology: case report. *Braz Dent J*, 15, 3, (March 2004), pp. (243-247)

Dattilo DJ & Bursick D. (1994). Management of traumatic cranial vault deformities using three-dimensional computer-generated models. *J Trauma*, 36, 5, (May 1994), pp. (691-694)

D'Urso PS, Barker TM, Earwaker WJ, Bruce LJ, Atkinson RL, Lanigan MW, Arvier JF & Effeney DJ. (1999). Stereolithographic biomodelling in cranio-maxillofacial surgery: a prospective trial. *J Craniomaxillofac Surg* , 27, 1, (February 1999), pp. (30-37) ISSN 1010-5182

Eisele DW, Richtsmeier WJ, Graybeal JC, Koch WM & Zinreich SJ. (1994). Three-dimensional models for head and neck tumor treatment planning. *Laryngoscope*, 104, 4, (April 1994), pp. (433-439) ISSN 0023-852X

Ekstrand K & Hirsch JM. (2008). Malignant tumors of the maxilla: virtual planning and real-time rehabilitation with custom-made R-zygoma fixtures and carbon-graphite fiber-reinforced polymer prosthesis. *Clin Implant Dent Relat Res*, 10, 1, (March 2008), pp. (23-29) ISSN 1523-0899

Epker BN, & Wolford LM. (1980). *Dentofacial deformities. Surgical-orthodontic correction* CV Mosby, ISBN 0801616069, St Louis, Toronto, London

Ewers R & Schicho K. (2009). Augmented reality telenavigation in cranio maxillofacial oral surgery. *Stud Health Technol Inform*, 150, pp. (24-25)

Ewers R, Schicho K, Undt G, Wanschitz F, Truppe M, Seemann R & Wagner A. (2005). Basic research and 12 years of clinical experience in computer-assisted navigation technology: a review. *Int J Oral Maxillofac Surg*, 34, 1, (January 2005), pp. (1-8)

Fariña R, Plaza C & Martinovic G. (2009). New transference technique of position of mandibular reconstructing plates using stereolithographic models. *J Oral Maxillofac Surg*, 67, 11, (November 2009), pp. (2544-2548)

Feiyun P, Wei L, Jun C, Xin X, Zhuojin S & Fengguo Y. (2010). Simultaneous correction of bilateral temporomandibular joint ankylosis with mandibular micrognathia using internal distraction osteogenesis and 3-dimensional craniomaxillofacial models. *J Oral Maxillofac Surg*, 68, 3, (March 2010), pp. (571-577)

Frühwald J, Schicho KA, Figl M, Benesch T, Watzinger F & Kainberger F. (2008). Accuracy of craniofacial measurements: computed tomography and three-dimensional computed tomography compared with stereolithographic models. *J Craniofac Surg*, 19, 1, (January 2008), pp. (22-26) ISSN 1049-2275

Gateno J, Xia JJ, Teichgraeber JF, Christensen AM, Lemoine JJ, Liebschner MA, Gliddon MJ & Briggs ME. (2007). Clinical feasibility of computer-aided surgical simulation (CASS) in the treatment of complex cranio-maxillofacial deformities. *J Oral Maxillofac Surg*, 65, 4, (April 2007), pp. (728-734)

Gosain AK, Santoro TD, Havlik RJ, Cohen SR & Holmes RE. (2002). Midface distraction following Le Fort III and monobloc osteotomies: problems and solutions. *Plast Reconstr Surg*, 109, 6, (May 2002), pp. (1797-1808) ISSN 0032-1052

He Y, Zhu HG, Zhang ZY, He J & Sader R. (2009). Three-dimensional model simulation and reconstruction of composite total maxillectomy defects with fibula osteomyocutaneous flap flow-through from radial forearm flap. *Oral Surg Oral Med Oral Pathol Oral Radiol Endod*, 108, 6, (December 2009), pp. (e6-12)

Hibi H, Sawaki Y & Ueda M. (1997). Three-dimensional model simulation in orthognathic surgery. *Int J Adult Orthodon Orthognath Surg*, 12, 3, pp. (226-232) ISSN 0742-1931

Hirsch DL, Garfein ES, Christensen AM, Weimer KA, Saddeh PB & Levine JP. (2009). Use of computer-aided design and computer-aided manufacturing to produce orthognathically ideal surgical outcomes: a paradigm shift in head and neck reconstruction. *J Oral Maxillofac Surg*, 67, 10, (October 2009), pp. (2115-2122)

Hoffmann J, Schwaderer E & Dammann F. (2002). The use of hybrid stereolithographic models for the planning of complex craniofacial procedures. Biomed Tech (Berl), 47, Suppl 1 Pt 1, pp. (278-281)

Husami T, Leffler K, Churnik R & Lehman JA Jr. (1988). Sterilization of the bone pencil. *Plast Reconstruct Surg*, 82, 6, (December 1988), p. (1100)

Ibrahim D, Broilo TL, Heitz C, de Oliveira MG, de Oliveira HW, Nobre SM, Dos Santos Filho JH & Silva DN. (2009). Dimensional error of selective laser sintering, three-dimensional printing and PolyJet models in the reproduction of mandibular anatomy. *J Craniomaxillofac Surg*, 37, 3, (April 2009), pp. (167-173)

Jakab K, Norotte C, Marga F, Murphy K, Vunjak-Novakovic G & Forgacs G. (2010). Tissue engineering by self-assembly and bio-printing of living cells. *Biofabrication*, 2, 2 (June 2010), 022001. doi: 10.1088/1758-5082/2/2/022001

Jeelani NU, Khan MA, Fitzgerald O'Connor EJ, Dunaway D & Hayward R. (2009). Frontofacial monobloc distraction using the StealthStation intraoperative navigation system: the ability to see where you are cutting. *J Craniofac Surg*, 20, 3, (May 2009), pp. (892-894)

Juergens P, Krol Z, Zeilhofer HF, Beinemann J, Schicho K, Ewers R & Klug C. (2009). Computer simulation and rapid prototyping for the reconstruction of the mandible. *J Oral Maxillofac Surg*, 67, 10, (October 2009), pp. (2167-2170)

Kermer C, Lindner A, Friede I, Wagner A & Millesi W. (1998). Preoperative stereolithographic model planning for primary reconstruction in craniomaxillofacial trauma surgery. *J Craniomaxillofac Surg*, 26, 3, (June 1998), pp. (136-139) ISSN 1010-5182

Kermer C, Rasse M, Lagogiannis G, Undt G, Wagner A & Millesi W. (1998). Colour stereolithography for planning complex maxillofacial tumour surgery. *J Craniomaxillofac Surg*, 26, 6, (December 1998), pp. (360-362) ISSN 1010-5182

Kernan BT & Wimsatt JA 3rd. (2000). Use of a stereolithography model for accurate, preoperative adaptation of a reconstruction plate. *J Oral Maxillofac Surg*, 58, 3, (March 2000), pp. (349-351) ISSN 0278-2391

Klammert U, Böhm H, Schweitzer T, Würzler K, Gbureck U, Reuther J & Kübler A. (2009). Multi-directional Le Fort III midfacial distraction using an individual prefabricated device. *J Craniomaxillofac Surg*, 37, 4, (June 2009), pp. (210-215)

Klug C, Schicho K, Ploder O, Yerit K, Watzinger F, Ewers R, Baumann A & Wagner A. (2006). Point-to-point computer-assisted navigation for precise transfer of planned zygoma osteotomies from the stereolithographic model into reality. J Oral Maxillofac Surg, 64, 3, (March 2006), pp. (550-559)

Korves B, Klimek L, Klein HM & Mösges R. (1995). Image- and model-based surgical planning in otolaryngology. *J Otolaryngol* 24, 5, (October 1995), pp. (265-270) ISSN 0381-6605

Kozakiewicz M, Elgalal M, Loba P, Komunski P, Arkuszewski P, Broniarczyk-Loba A & Stefanczyk L. (2009). Clinical application of 3D pre-bent titanium implants for orbital floor fractures. *J Craniomaxillofac Surg*, 37, 4, (June 2009), pp. (229-234)

Kragskov J, Sindet-Pedersen S, Gyldensted C & Jensen KL. (1996). A comparison of three-dimensional computed tomography scans and stereolithographic models for evaluation of craniofacial anomalies. *J Oral Maxillofac Surg*, 54, 4, (April 1996), pp. (402-411, discussion 411-412) ISSN 0278-2391

Kübler N, Michel C, Zöller J, Bill J, Mühling J & Reuther J. (1995). Repair of human skull defects using osteoinductive bone alloimplants. *J Craniomaxillofac Surg*, 23, pp. (337-346) ISSN 1010-5182

Leiggener C, Messo E, Thor A, Zeilhofer HF & Hirsch JM. (2009). A selective laser sintering guide for transferring a virtual plan to real time surgery in composite mandibular reconstruction with free fibula osseous flaps. *Int J Oral Maxillofac Surg*, 38, 2, (February 2009), pp. (187-192)

Lethaus B, Kessler P, Boeckman R, Poort LJ & Tolba R. (2010). Reconstruction of a maxillary defect with a fibula graft and titanium mesh using CAD/CAM techniques. *Head Face Med*, 19, 6, (July 2010), 16

Li WZ, Zhang MC, Li SP, Zhang LT & Huang Y. (2009). Application of computer-aided three-dimensional skull model with rapid prototyping technique in repair of

zygomatico-orbito-maxillary complex fracture. *Int J Med Robot*, 5, 2, (June 2009), pp. (158-163)

Liu XJ, Gui L, Mao C, Peng X & Yu GY. (2009). Applying computer techniques in maxillofacial reconstruction using a fibula flap: a messenger and an evaluation method. *J Craniofac Surg*, 20, 2, (March 2009), pp. (372-377)

Lo LJ & Chen YR. (2003). Three-dimensional computed tomography imaging in craniofacial surgery: morphological study and clinical applications. *Chang Gung Med J*, 26, 1, (January 2003), pp. (1-11) ISSN 0255-8270

Lo LJ, Chen YR, Tseng CS & Lee MY. (2004). Computer-aided reconstruction of traumatic fronto-orbital osseous defects: aesthetic considerations. *Chang Gung Med J*, 27, 4, (April 2004), pp. (283-291) ISSN 0255-8270

Mainenti P, Oliveira GS, Valério JB, Daroda LS, Daroda RF, Brandão G & Rosa LE. (2009). Ameloblastic fibro-odontosarcoma: a case report. *Int J Oral Maxillofac Surg*, 38, 3, (March 2009), pp. (289-292)

Mankovich NJ, Samson D, Pratt W, Lew D & Beumer J 3rd. (1994). Surgical planning using three-dimensional imaging and computer modeling. *Otolaryngol Clin North Am*, 27, 5, (October 1994), pp. (875-889) ISSN 0030-6665

Matsumoto K, Nakanishi H, Seike T, Koizumi Y & Hirabayashi S. (2003). Intracranial hemorrhage resulting from skull base fracture as a complication of Le Fort III osteotomy. *J Craniofac Surg*, 14, 4, (July 2003), pp. (545-548) ISSN 1049-2275

Matsuo A, Chiba H, Takahashi H, Toyoda J & Abukawa H. (2010). Clinical application of a custom-made bioresorbable raw particulate hydroxyapatite/poly-L-lactide mesh tray for mandibular reconstruction. *Odontology*, 98, 1, (February 2010), pp. (85-88)

Mavili ME, Canter HI, Saglam-Aydinatay B, Kamaci S & Kocadereli I. (2007). Use of three-dimensional medical modeling methods for precise planning of orthognathic surgery. *J Craniofac Surg*, 18, 4, (July 2007), pp. (740-747) ISSN 1049-2275

Minami K, Mori Y, Tae-Geon K, Shimizu H, Ohtani M & Yura Y. (2007). Maxillary distraction osteogenesis in cleft lip and palate patients with skeletal anchorage. *Cleft Palate Craniofac J*, 44, 2, (March 2007), pp. (137-141) ISSN 1055-6656

Mironov V, Kasyanov V & Markwald RR. (2011). Organ printing: from bioprinter to organ biofabrication line. *Curr Opin Biotechnol*, 16, (March 2011)

Mironov V, Boland T, Trusk T, Forgacs G & Markwald RR. (2003). Organ printing: computer-aided jet-based 3D tissue engineering. *Trends Biotechnol*, 21, 4, (April 2003), pp. (157-161)

Müller A, Krishnan KG, Uhl E & Mast G. (2003). The application of rapid prototyping techniques in cranial reconstruction and preoperative planning in neurosurgery. *J Craniofac Surg*, 14, 6, (November 2003), pp. (899-914) ISSN 1049-2275

Murray DJ, Edwards G, Mainprize JG & Antonyshyn O. (2008). Optimizing craniofacial osteotomies: applications of haptic and rapid prototyping technology. *J Oral Maxillofac Surg*, 66, 8, (August 2008), pp. (1766-1772)

Nakajima T, Yoshimura Y, Nakanishi Y, Koga S & Katada K. (1995). Integrated life-sized solid model of bone and soft tissue: application for cleft lip and palate infants. *Plast Reconstr Surg*, 96, 5, (October 1995), pp. (1020-1025) ISSN 0032-1052

Nout E, Cesteleyn LL, van der Wal KG, van Adrichem LN, Mathijssen IM & Wolvius EB. (2008). Advancement of the midface, from conventional Le Fort III osteotomy to Le

Fort III distraction: review of the literature. *Int J Oral Maxillofac Surg*, 37, 9, (September 2008), pp. (781-789)

Olszewski R, Tranduy K & Reychler H. (2010). Innovative procedure for computer-assisted genioplasty: three-dimensional cephalometry, rapid prototyping model and surgical splint. *Int J Oral maxillofac Surg*, 39, 7, (July 2010), pp. (721-724)

Olszewski R, Tran Duy K, Raucent B, Hebda A & Reychler H.(2008). Communicating a clinical problem to the engineers: towards a common methodology. *Int J Oral Maxillofac Surg*, 37, 3, (March 2008), pp. (269-274)

Olszewski R, Reychler H, Cosnard G, Denis JM, Vynckier S & Zech F. (2008). Accuracy of three-dimensional (3D) craniofacial cephalometric landmarks on a low-dose 3D computed tomograph. *Dentomaxillofac Radiol*, 37, 5, (July 2008), pp. (261-267)

Olszewski R, Zech F, Cosnard G, Nicolas V, Macq B & Reychler H. (2007). 3D CT cephalometric craniofacial analysis: Experimental validation in vitro. *Int J Oral Maxillofac Surg*, 36, 9, (September 2007), pp. (828-833)

Ono I, Gunji H, Suda K & Kaneko F. 1(994). Method for preparing an exact-size model using helical volume scan computed tomography. *Plast Reconstr Surg*, 93, 7, (June 1994), pp. (1363-1371) ISSN 0032-1052

Ortakoglu K, Akcam T, Sencimen M, Karakoc O, Ozyigit HA & Bengi O. (2007). Osteochondroma of the mandible causing severe facial asymmetry: a case report. *Oral Surg Oral Med Oral Pathol Oral Radiol Endod*, 103, 5, (May 2007), pp. (e21-e28)

Papadopoulos MA, Christou PK, Christou PK, Athanasiou AE, Boettcher P, Zeilhofer HF, Sader R & Papadopulos NA. (2002). Three-dimensional craniofacial reconstruction imaging. *Oral Surg Oral Med Oral Pathol Oral Radiol Endod*, 93, 4, (April 2002), pp. (382-393)

Pelo S, Tassiello S, Boniello R, Gasparini G & Longobardi G. (2006). A new method for assessment of craniofacial malformations. *J Craniofac Surg*, 17, 6, (November 2006), pp. (1035-1039) ISSN 1049-2275

Poukens J, Haex J & Riediger D. (2003). The use of rapid prototyping in the preoperative planning of distraction osteogenesis of the cranio-maxillofacial skeleton. *Comput Aided Surg*, 8, 3, pp. (146-154) ISSN 1092-9088

Powers DB, Edgin WA & Tabatchnick L. (1998). Stereolithography: a historical review and indications for use in the management of trauma. *J Craniomaxillofac Trauma*, 4, 3, (Fall 1998), pp. (16-23)

Robiony M. (2010). Distraction osteogenesis: a method to improve facial balance in asymmetric patients. *J Craniofac Surg*, 21, 2, (March 2010), pp. (508-512)

Robiony M, Salvo I, Costa F, Zerman N, Bazzocchi M, Toso F, Bandera C, Filippi S, Felice M & Politi M. (2007). Virtual reality surgical planning for maxillofacial distraction osteogenesis: the role of reverse engineering rapid prototyping and cooperative work. *J Oral Maxillofac Surg*, 65, 6, (June 2007), pp. (1198-1208)

Rotaru H, Baciut M, Stan H, Bran S, Chezan H, Iosif A, Tomescu M, Kim SG, Rotaru A & Baciut G. (2006). Silicone rubber mould cast polyethylmethacrylate-hydroxyapatite plate used for repairing a large skull defect. *J Craniomaxillofac Surg*, 34, 4, (June 2006), pp. (242-246)

Sailer HF, Haers PE, Zollikofer CP, Warnke T, Carls FR & Stucki P. (1998). The value of stereolithographic models for preoperative diagnosis of craniofacial deformities

and planning of surgical corrections. *Int J Oral Maxillofac Surg*, 27, 5, (October 1998), pp. (327-333)

Sannomiya EK, Reis SA, Asaumi J, Silva JV, Barbara AS & Kishi K. (2006). Clinical and radiographic presentation and preparation of the prototyping model for pre-surgical planning in Apert's syndrome. *Dentomaxillofac Radiol*, 35, 2, (March 2006), pp. (119-124)

Sannomiya EK, Silva JV, Brito AA, Saez DM, Angelieri F & Dalben Gda S. (2008). Surgical planning for resection of an ameloblastoma and reconstruction of the mandible using a selective laser sintering 3D biomodel. *Oral Surg Oral Med Oral Pathol Oral Radiol Endod*, 106, 1, (July 2008), pp. (e36-40)

Santler G, Karcher H & Ruda C. (1998). Indications and limitations of three-dimensional models in cranio-maxillofacial surgery. *J Craniomaxillofac Surg*, 26, 1, (February 1998), pp. (11-16) ISSN 1010-5182

Sato K, Sugawara J, Mitani H & Kawamura H. (1998). Use of selectively colored stereolithography for diagnosis of impacted supernumerary teeth for a patient with cleidocranial dysplasia. *Int J Adult Orthodon Orthognath Surg*, 13, 2, pp. (163-167)

Schicho K, Figl M, Seemann R, Ewers R, Lambrecht JT, Wagner A, Watzinger F, Baumann A, Kainberger F, Fruehwald J & Klug C. (2006). Accuracy of treatment planning based on stereolithography in computer assisted surgery. *Med Phys*, 33, 9, (September 2006), pp. (3408-3459) ISSN 0094-2405

Schon R, Metzger MC, Zizelmann C, Weyer N & Schmelzeisen R. (2006). Individually preformed titanium mesh implants for a true-to-original repair of orbital fractures. *Int J Oral Maxillofac Surg*, 35, 11, (November 2006), pp. (990-995)

Silva DN, Gerhardt de Oliveira M, Meurer E, Meurer MI, Lopes da silva JE & Santa-Barbara A. (2008). Dimensional error in selective laser sintering and 3D-printing of models for craniomaxillary anatomy reconstruction. *J Craniomaxillofac Surg*, 36, 8, (December 2008), pp. (443-449)

Sinn DP, Cillo JE Jr & Miles BA. (2006). Stereolithography for craniofacial surgery. *J Craniofac Surg*, 17, 5, (September 2006), pp. (869-875) ISSN 1049-2275

Sohmura T, Kusumoto N, Otani T, Yamada S, Wakabayashi K & Yatani H. (2009). CAD/CAM fabrication and clinical application of surgical template and bone model in oral implant surgery. *Clin Oral Implants Res*, 20, 1, (January 2009), pp. (87-93)

Song SJ, Choi J, Park YD, Lee JJ, Hong SY & Sun K. (2010). A three-dimensional bioprinting system for use with a hydrogel-based biomaterial and printing parameter characterization. *Artif Organs;*34, 11 (November 2010), pp. (1044-1048)

Scolozzi P, Momjian A, Heuberger J, Andersen E, Broome M, Terzic A & Jaques B. (2009). Accuracy and predictability in use of AO three-dimensionally preformed titanium mesh plates for posttraumatic orbital reconstruction: a pilot study. *J Craniofac Surg*, 20, 4, (July 2009), pp. (1108-1113)

Undt G, Wild K, Reuther G & Ewers R. (2000). MRI-based stereolithographic models of the temporomandibular joint: technical innovation. *J Craniomaxillofac Surg*, 28, 5, (October 2000), pp. (258-263) ISSN 1010-5182

Varol A & Basa S. (2009). The role of computer-aided 3D surgery and stereolithographic modelling for vector orientation in premaxillary and trans-sinusoidal maxillary distraction osteogenesis. *Int J Med Robot*, 5, 2, (June 2009), pp. (198-206)

Vrielinck L, Politis C, Schepers S, Pauwels M & Naert I. (2003). Image-based planning and clinical validation of zygoma and pterygoid implant placement in patients with severe bone atrophy using customized drill guides. Preliminary results from a prospective clinical follow-up study. *Int J Oral Maxillofac Surg*, 32, 1, (February 2003), pp. (7-14) ISSN 0901-5027

Wagner JD, Baack B, Brown GA & Kelly J. (2004). Rapid 3-dimensional prototyping for surgical repair of maxillofacial fractures: a technical note. *J Oral Maxillofac Surg*, 62, 7, (July 2004), pp. (898-901)

Whitman DH & Connaughton B. (1999). Model surgery prediction for mandibular midline distraction osteogenesis. *Int J Oral Maxillofac Surg*, 28, 6, (December 1999), pp. (421-423)

Williams JV & Revington PJ. (2010). Novel use of an aerospace selective laser sintering machine for rapid prototyping of an orbital blowout fracture. *Int J Oral Maxillofac Surg*, 39, 2, (February 2010), pp. (182-184)

Winder J & Bibb R. (2005). Medical rapid prototyping technologies: state of the art and current limitations for application in oral and maxillofacial surgery. *J Oral Maxillofac Surg*, 63, 7, (July 2005), pp. (1006-1015)

Wong TY, Fang JJ, Chung CH & Huang JS. (2002). Restoration of the temporal defect using laser stereolithography technique. *J Oral Maxillofac Surg*, 60, 11, (November 2002), pp. (1374-1376) ISSN 0278-2391

Wong TY, Fang JJ, Chung CH, Huang JS & Lee JW. (2005). Comparison of 2 methods of making surgical models for correction of facial asymmetry. J Oral Maxillofac Surg, 63, 2, (February 2005), pp. (200-208)

Worrall SF & Christensen RW. Alloplastic reconstruction of the temporomandibular joint in treatment of craniofacial developmental or congenital anomalies: a surgical case report. *Surg Technol Int*, 15, pp. (291-304) ISSN 1090-3941

Wu CT, Lee ST, Chen JF, Lin KL & Yen SH. (2008). Computer-aided design for three-dimensional titanium mesh used for repairing skull base bone defect in pediatric neurofibromatosis type 1. A novel approach combining biomodeling and neuronavigation. *Pediatr Neurosurg*, 44, 2, (January 2008), pp. (133-139) ISSN 1016-2291

Xia J, Ip HH, Samman N, Wang D, Kot CS, Yeung RW & Tideman H. (2000). Computer-assisted three-dimensional surgical planning and simulation: 3D virtual osteotomy. *Int J Oral Maxillofac Surg* 29, 1, (February 2000), pp. (11-17) ISSN 0901-5027

Yamaji KE, Gateno J, Xia JJ & Teichgraeber JF. (2004). New internal Le Fort I distractor for the treatment of midface hypoplasia. *J Craniofac Surg*, 15, 1, (January 2004), 124-127 ISSN 1049-2275

Yamashita Y, Yamaguchi Y, Tsuji M, Shigematsu M & Goto M. (2008). Mandibular reconstruction using autologous iliac bone and titanium mesh reinforced by laser welding for implant placement. *Int J Oral Maxillofac Implants*, 23, 6, (November-December 2008), pp. (1143-1146)

Yau YY, Arvier JF & Barker TM. (1995). Technical note: maxillofacial biomodelling--preliminary result. *Br J Radiol*, 68, 809, (May 1995), pp. (519-523) ISSN 0007-1285

Zhang S, Liu X, Xu Y, Yang C, Undt G, Chen M, Haddad MS & Yun B. (2011). Application of rapid prototyping for temporomandibular joint reconstruction. *J Oral Maxillofac Surg*, 69, 2, (February 2011), pp. (432-438)

Zhou L, He L, Shang H, Liu G, Zhao J & Liu Y. (2009). Correction of hemifacial microsomia with the help of mirror imaging and a rapid prototyping technique: case report. *Br J Oral Maxillofac Surg*, 47, 6, (September 2009), pp. (486-488)

Zhou LB, Shang HT, He LS, Bo B, Liu GC, Liu YP & Zhao JL. (2010). Accurate reconstruction of discontinuous mandible using a reverse engineering/computer-aided design/rapid prototyping technique: a preliminary clinical study. *J Oral Maxillofac Surg*, 68, 9, (September 2010), pp. (2115-2121)

Zizelmann C, Bucher P, Rohner D, Gellrich NC, Kokemueller H & Hammer B. (2010). Virtual restoration of anatomic jaw relationship to obtain a precise 3D model for total joint prosthesis construction for treatment of TMJ ankylosis with open bite. *Int J Oral Maxillofac Surg*, 39, 10, (October 2010), pp. (1012-1015)

IntechOpen

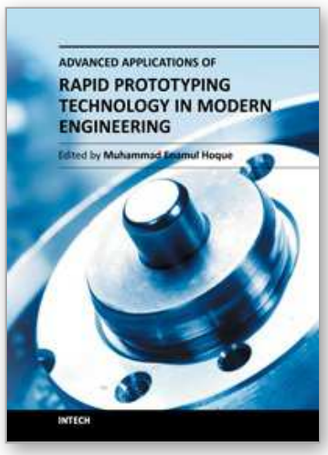

Advanced Applications of Rapid Prototyping Technology in Modern Engineering

Edited by Dr. M. Hoque

ISBN 978-953-307-698-0
Hard cover, 364 pages
Publisher InTech
Published online 22, September, 2011
Published in print edition September, 2011

Rapid prototyping (RP) technology has been widely known and appreciated due to its flexible and customized manufacturing capabilities. The widely studied RP techniques include stereolithography apparatus (SLA), selective laser sintering (SLS), three-dimensional printing (3DP), fused deposition modeling (FDM), 3D plotting, solid ground curing (SGC), multiphase jet solidification (MJS), laminated object manufacturing (LOM). Different techniques are associated with different materials and/or processing principles and thus are devoted to specific applications. RP technology has no longer been only for prototype building rather has been extended for real industrial manufacturing solutions. Today, the RP technology has contributed to almost all engineering areas that include mechanical, materials, industrial, aerospace, electrical and most recently biomedical engineering. This book aims to present the advanced development of RP technologies in various engineering areas as the solutions to the real world engineering problems.

How to reference

In order to correctly reference this scholarly work, feel free to copy and paste the following:

Olszewski Raphael and Reychler Herve (2011). Clinical Applications of Rapid Prototyping Models in Cranio-Maxillofacial Surgery, Advanced Applications of Rapid Prototyping Technology in Modern Engineering, Dr. M. Hoque (Ed.), ISBN: 978-953-307-698-0, InTech, Available from: http://www.intechopen.com/books/advanced-applications-of-rapid-prototyping-technology-in-modern-engineering/clinical-applications-of-rapid-prototyping-models-in-cranio-maxillofacial-surgery

INTECH
open science | open minds

InTech Europe
University Campus STeP Ri
Slavka Krautzeka 83/A
51000 Rijeka, Croatia
Phone: +385 (51) 770 447
Fax: +385 (51) 686 166
www.intechopen.com

InTech China
Unit 405, Office Block, Hotel Equatorial Shanghai
No.65, Yan An Road (West), Shanghai, 200040, China
中国上海市延安西路65号上海国际贵都大饭店办公楼405单元
Phone: +86-21-62489820
Fax: +86-21-62489821

© 2011 The Author(s). Licensee IntechOpen. This chapter is distributed under the terms of the Creative Commons Attribution-NonCommercial-ShareAlike-3.0 License, which permits use, distribution and reproduction for non-commercial purposes, provided the original is properly cited and derivative works building on this content are distributed under the same license.

IntechOpen

IntechOpen